

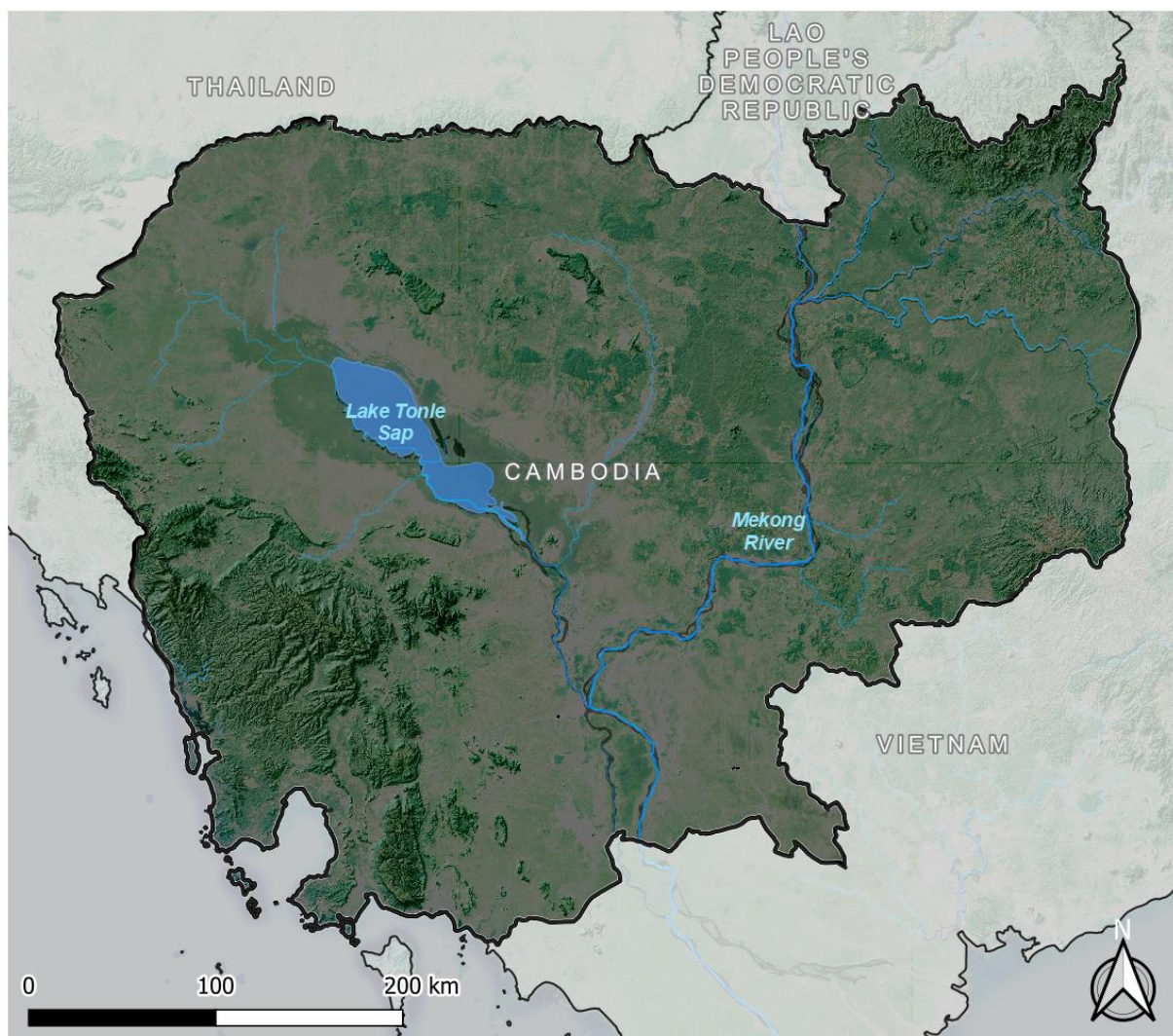
Spatial Screening of Climate-related Natural Hazards in Cambodia

Prepared by A. H. Essenfelder and M. Amadio

I Introduction

Cambodia is a country located in Southeastern Asia and bordering the Gulf of Thailand, between the bordering countries of Thailand, Vietnam, and Laos. It has a total area of about 181,000 km², out of which water represents 4,520 km², mostly due to the large Tonle Sap Lake, the largest freshwater lake in southeast Asia, located in the central-western part of the country (*Figure 1*). Another important water body is the Mekong River, which crosses the country from north-east to the south and is shared with regional neighboring countries (China, Burma, Thailand, Laos, and Vietnam).

Figure 1: Natural map of Cambodia with main water bodies

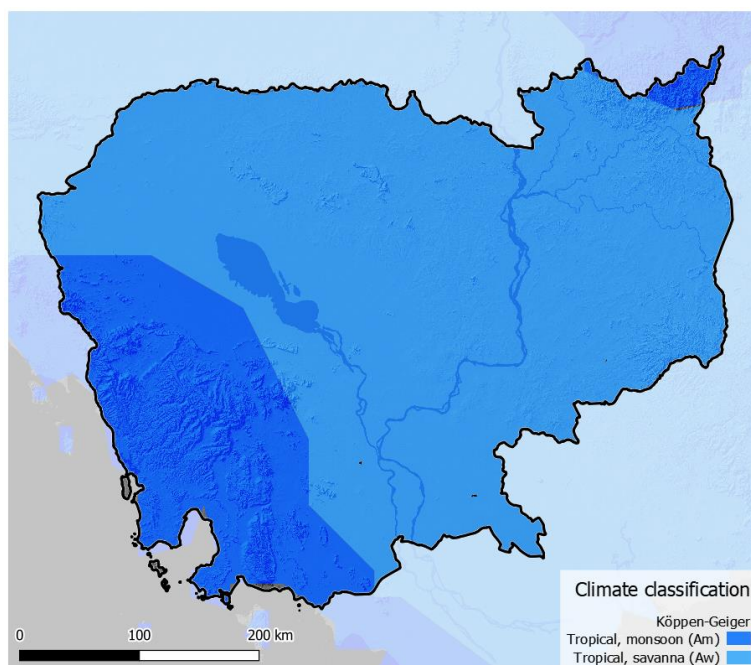


The landscape of Cambodia is largely dominated by paddies and forests around the central plains of Mekong River and the Lake Tonle Sap, while mountain ranges can be found in the north-eastern and south-western parts of the country (Elephant or Dâmbrei mountains and Cardamom or Krâvanh mountains, hosting the highest point of the country at Phnum Aoral, 1,810 m). Cambodia is a

predominantly rural country: in agricultural land accounts for about one third of the total extent (32.1%; from this total, 22.7% represents arable land, 0.9% permanent crops, and 8.5% permanent pastures). Forests cover the majority of the country (56.5%), while the remaining 11.4% consists of urban settlements (about 1% of total), shrublands, and wetlands ([The World Factbook, 2022](#)).

Cambodia presents mainly two different climate zones which reflect its different geography and the contrasts between the central flatlands and paddies to the bordering mountain regions (*Figure 2*). The southern-western and a small part of the north-eastern part of the country is influenced by the monsoons originating from the Indian Ocean, with a rainy, monsoon season between May to November and a dry season from December to April. Monsoonal rains, usually more intense during the months of June to November, often leads to flooding, while occasional droughts can also be observed during the crop growing season. The average rainfall is typically about 1,400-2,000 mm per year, with higher rates over coastal and highland areas. Inter-annual precipitation variability can be attributed to the El Niño Southern Oscillation (ENSO), which affects monsoon patterns over all the South-East Asia region. Negative ENSO events generally bring warmer and drier than average winter conditions across Southeast Asia, while positive ENSO episodes bring cooler than average conditions ([WB CCKP, 2022](#)). In terms of average annual temperatures, Cambodia is subject to little seasonal temperature variation, and average temperatures are relatively uniform across the country, reaching its highest values (often exceeding 32°C) during the early summer months before the rainy season begins. Temperatures remain between 25-27°C throughout the rest of the year.

Figure 2: Köppen-Geiger climate classification of Cambodia

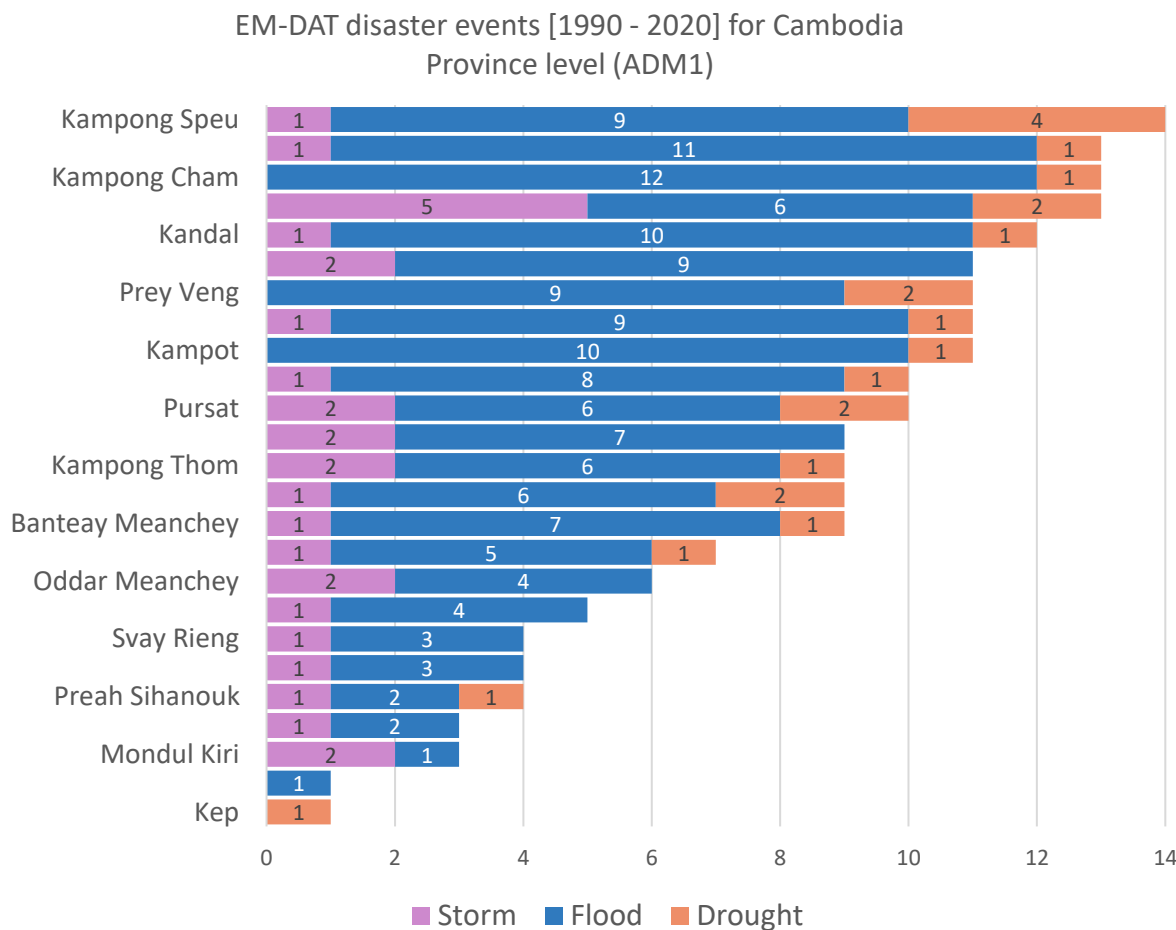


In an economic context, Cambodia has experienced strong economic growth over the last couple of decades (average annual GDP growth rate of over 8% between 2000-2010 and about 7% since 2011). The tourism, construction, agriculture, and textiles are the main sectors responsible for the bulk of economic growth. About 700,000 people, the majority of whom are women, are employed in the textile and clothing sectors, while an additional 500,000 people are employed in the tourism sector ([WBG, 2022a](#)). Due to its rapid economic growth, Cambodia is strongly affected by migration, particularly internal migration driven by people's search for work, education, and better socio-economic conditions. Rural-to-urban migration is the most common, followed by rural-to-rural

migration across different regions of the country. Urban migration focuses on the pursuit of unskilled or semi-skilled jobs in Phnom Penh, the capital city of Cambodia, with men working mainly in the construction industry and women working in garment factories. Migration, however, can also be triggered by natural hazards and extreme weather events ([Parsons and Nielsen, 2020](#); [Oudry et al., 2016](#)).

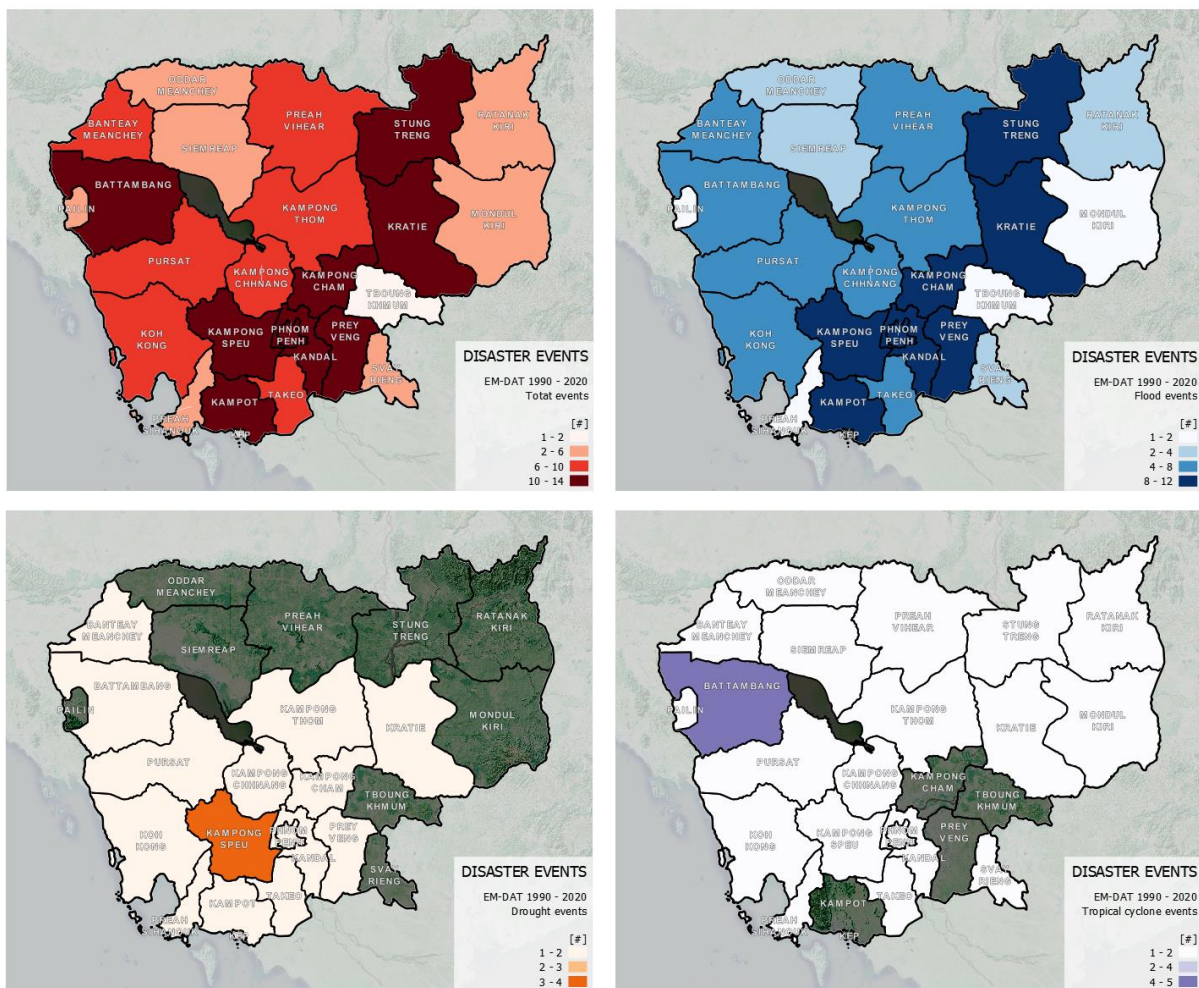
Cambodia is historically affected by extreme weather events, particularly droughts and flooding; landslides and tropical cyclones are not uncommon in the country as well. The count of extreme events as recorded in EM-DAT in Cambodia per District between 1990 and 2022 is shown in *Figure 3*. The long-term Climate Risk Index (CRI) ranks Cambodia as the 84th most at-risk country over the 2000-2019 period ([CRI 2021](#)). Under the longer-term perspective, climate change projections and their forecasted impact on people and the economy are concerning for the country's economy ([WBG, 2022b](#)). According to EM-DAT ([2022](#)), 39 disasters occurred in the last 32 years; 25 of them were related to flooding triggered by heavy precipitation, especially during the monsoon and the typhoon season. Major flooding events affect a significant amount of population and occur in average every five years (e.g. 1961, 1966, 1978, 1984, 1991, 1996, 2000, 2001 and 2002). One of the worst floods in Cambodia's history has occurred in year 2000 when 750,618 families (representing over 3 million people) have been estimated to be temporarily evacuated from their homes and villages for a total physical damage estimated at USD 150 million. In 2001, floods caused the death of at least 62 people for an additional estimated USD 20 million damages.

Figure 3: disaster events reported by EM-DAT between 1990 and 2022 for Cambodia at ADM1 level



Since 1997, seven tropical cyclones (typhoons) were recorded to affect the country: Linda (1997), Ketsana (2009), Mirinae (2009), Vamco (2015), Linfa (2020), Noul (2020) and Noru (2022) ([EM-DAT, 2022](#)). The most recent disaster is the Tropical Cyclone Noru in September 2022, that has particularly affected northern Cambodia (Bântéay Méanchey, Otdar Mean Chey, Preah Vihear, Siemréab, Stœng Trêng) and killed 16 people. Many houses were flooded, a number of roads were damaged, and landslides triggered by intense rainfall have contributed to major damages, including sections of National Road 9 ([AHA Centre, 2022](#)).

Figure 4: maps of disaster events reported by EM-DAT between 1990 and 2022 for Cambodia at ADM1 level



With regards to droughts, six major events are listed by EM-DAT ([2022](#)), occurring in 1987, 1994, 2001, 2002, 2005 and 2016. In 2002, an unusually dry weather during the rainy season affected some 420 communes in 76 districts located in 10 provinces (Prey Veng, Kandal, Kampong Speu, Takeo, Svay Rieng, Kampong Thom, Kampong Cham, Kratie, Odor Meancheay and Banteay Meancheay). The event impacted over 2 million people and is estimated to have caused over USD 21.50 million in damages ([RGC, 2007](#)). Given that 76% of Cambodia's population currently lives in rural areas and agriculture constitutes 25% its of GDP and 49% of its labour force, drought is a major source of concern for the country ([WBG 2021a](#)).

In addition to tropical cyclones, floods, and droughts, Cambodia is also at risk of extreme heat stress. Climate models, such as the RCP 8.5 scenario, predict frequent heat waves over most of land the land mass, as temperatures are expected to rise rising up to 3.1 °C by 2090 ([WBG, 2022](#)). Poorer communities operating at subsistence level and reliant on rain-fed agriculture are expected to be most

adversely impacted by these events, as extreme temperatures will damage agricultural yields ([WBG, 2021](#)).

According to DesInventar ([2022](#)), flooding (1,243 deaths), tropical cyclones (1,191 deaths), and wildfires (184 deaths) are the leading causes of mortality due to natural hazards. Tropical cyclones (56,244 buildings), flooding (34,211), and wildfires (6,203) also cause the most number of structural damages to buildings in Cambodia. Overall, Cambodia's per-capita GDP, under scenarios RCP 2.6 and RCP 8.5, is projected to fall by 0.74% to 1.84% by the end of the century due to the effects of climate change ([Kahn et al. 2019](#)) and adversely impact its GDP by nearly 10% by 2050 ([WBG, 2021](#)). Cambodia is also runs the risk of a credit downgrade induced by climate change impacts ([Moody's Investors Service, 2021](#)).

These climate risks are however unevenly distributed across the country and depend on the probability and intensity with which a hazard occurs, the exposure to peoples and their assets, and their vulnerability to various hazard. In general, poorer households are least resilient to climate affects because they tend to reside in more disadvantaged and hazard-prone areas, have lower access to critical services like health, education and early warning systems, and their assets ([Hallegatte et al. 2018](#)). Per World Bank's estimates, 2.8 million people (17.8%) live below the poverty line in 2019 (World Bank, [2022](#)). This report provides an overview of exposure and risks associated with flooding (riverine and coastal), tropical cyclones, droughts, heat stress, landslides and air pollution, across Cambodia, with a special focus on the climate induced disaster risk on its poorest communities.

2 Definitions and Methodology

2.1 Disaster Risk

Disaster risk is the probability of a negative impact caused by a natural hazard. The Intergovernmental Panel on Climate Change (IPCC) defines natural hazard as potential events or trends that may cause loss of life, injury, or other health impacts, and damage and losses to property, infrastructure, livelihoods, service provision, ecosystems and environmental resources ([IPCC 2019 et al.](#)). Exposure characterizes the location of people and their assets which may be threatened by natural hazards. While people (and their assets) may get exposed, they may not be adversely impacted by hazards if they are not vulnerable. Together, hazard (**H**), exposure (**E**), and vulnerability (**V**) drive disaster risk (**R**) ([IPCC 2012](#)):

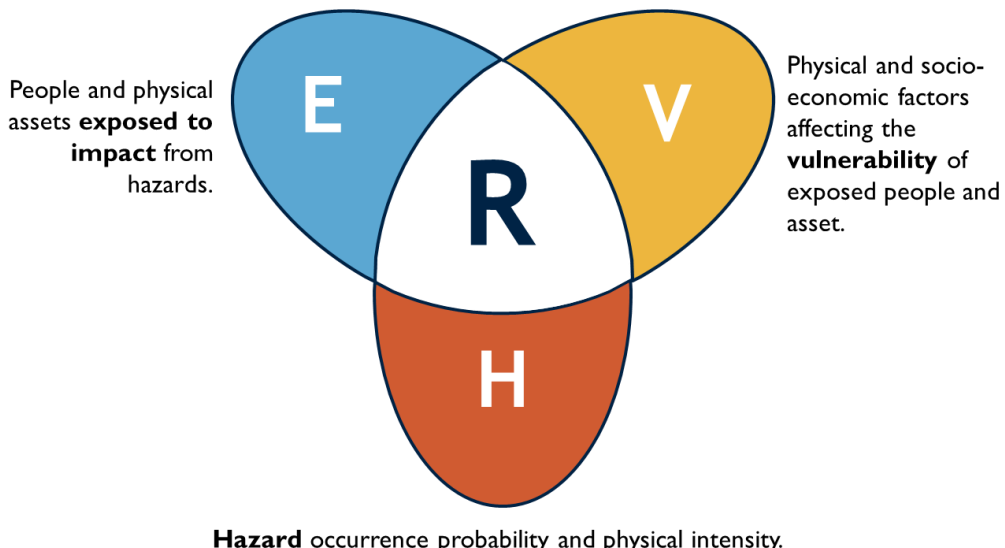
$$R=f(H, E, V)$$

➤ Example 1:

Risk (**R**) from floods (**H**) over population (**E**) according to water depth-mortality function (**V**).

➤ Example 2:

Risk (**R**) from strong winds (**H**) over built-up (**E**) according to wind-damage function (**V**).

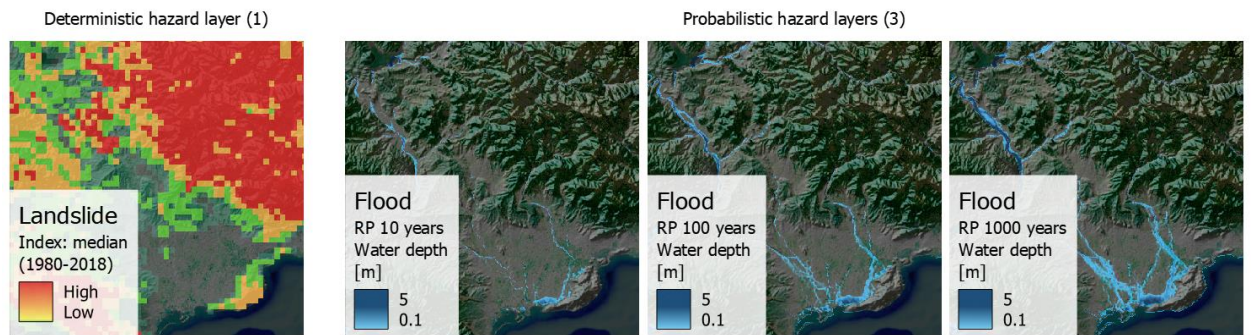


2.2 Hazard

Historical hazards (baseline) can be modelled in one of two following ways:

- a. Deterministic, in the form of an individual geodata layer measuring the mean, median or maximum intensity of a hazard aggregating historical data and modeling. This is the case for landslide and drought hazard (panel 1, figure 5)
- b. Probabilistic, in the form of multiple geodata layers, each representing a range of hazard physical intensities (e.g. water depth [metres], wind speed [kilometers per hour]) corresponding to a specific occurrence frequency, measured as Return Period (RP), in years. This is the case for river flood, coastal flood and strong winds (panel 2, figure 5)

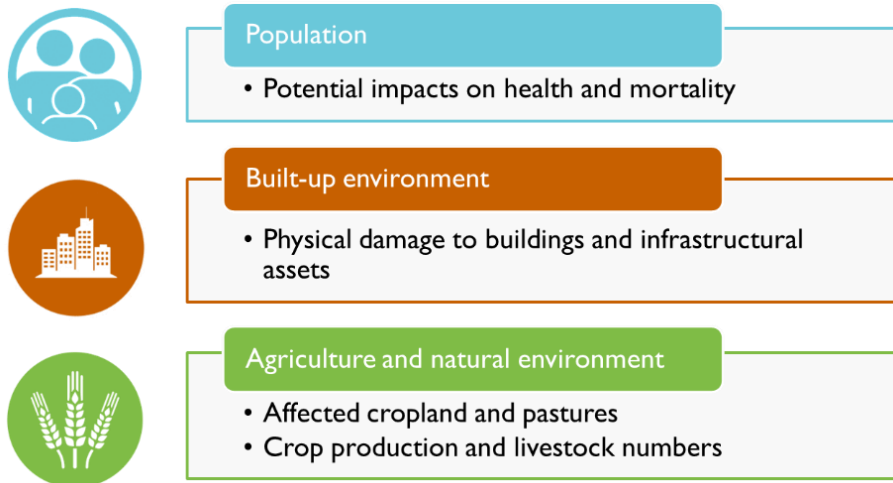
Figure 5: examples of individual deterministic hazard layer (landslide index) versus multiple probabilistic hazard layers (flood depth for three return periods of increasing intensity/decreasing frequency; RP stands for Return Period).



2.3 Exposure

Exposure describes the location of people and assets that are prone to suffer an impact from natural hazards. We consider three exposure categories used as main indicators of risk, listed in figure 6.

Figure 6: exposure categories considered in the analysis and related impact types



Each indicator is quantified by a specific spatial metric: *population* is described in terms of total count and as share of total population within an administrative unit, while *built-up* and *agricultural land* environment are measured in terms of area (hectares) and share over total land area within the administrative unit.

2.4 Vulnerability

Vulnerability is determined by physical, social, economic, and environmental factors or processes, which increase the susceptibility of an individual, their assets or a community, to hazards (UNDRR). Two main components of vulnerability are typically accounted for in this note:

Impact models, draw the relationship between the intensity of hazard and the predisposition of damage suffered by specific exposed categories into actual impact; e.g., a flood depth of 0.5m is expected to cause a low degree of impact in terms of population mortality, while a 3m flood would cause severe impact. Impact models can be quantitative, providing an absolute or relative estimate of the damage (i.e., in terms of USD or % of total value); or qualitative, classifying the impact in nominal categories.

Socio-economic conditions: Describe the differential susceptibility of exposed categories to suffer damage, i.e., areas under poverty conditions and high dependency rate are more likely to suffer damage compared to wealthy communities, under the same hazard event. These are measured using spatial indices based on demographics (sex, age composition, dependency rate) and socioeconomic statistics (wealth, GDP and average salary, among others), and are semi-quantitative metrics (index score; ranking)

Not all exposure categories are affected in the same way by physical hazards - some hazards are more relevant for one category than another. The impact model needs to be aligned with the hazard intensity metric, with the exposure category, and with the socio-economic conditions to which they are applied to. For this reason, the availability of such models dictates the possible combinations of hazard and exposure categories. As no country- or sub-country-specific impact functions are available for Cambodia, we rely on the utilization of global- or regional-level impact functions. *Table 1* identifies which combinations are sustained by currently available impact models, highlighted in magenta. Where no impact models are available, a simple exposure model is produced based on literature studies, highlighted in cyan.

Table 1: Available Hazard, Exposure, and Vulnerability components for Cambodia

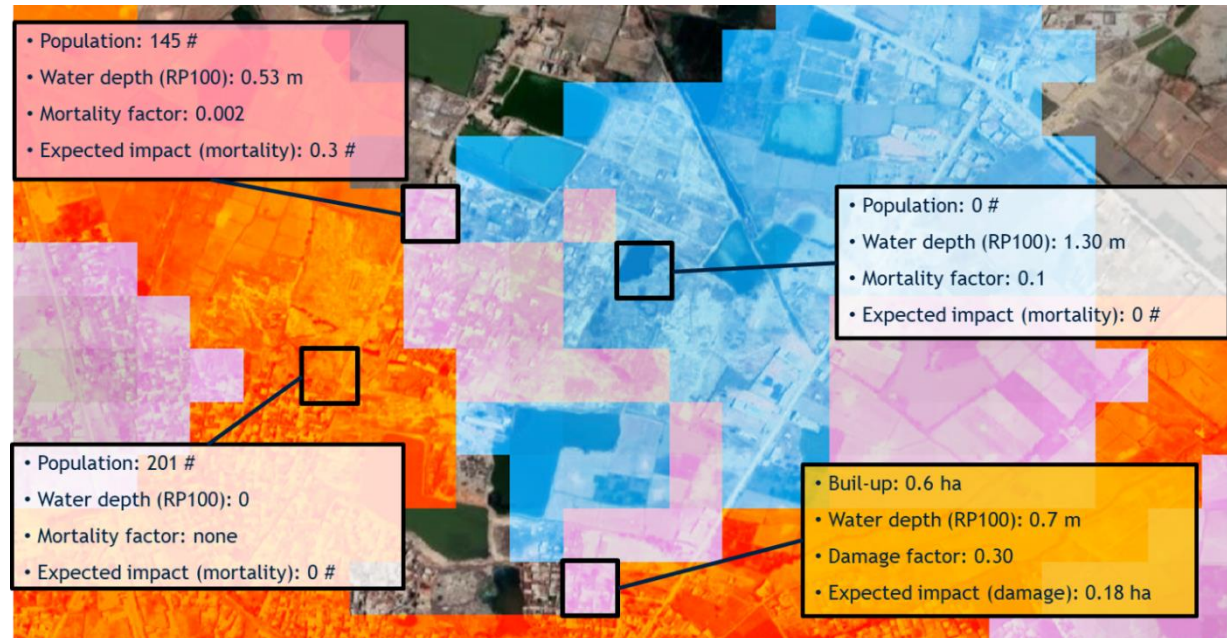
Hazard types	Exposure categories		
	Population (Mortality)	Built-up assets (Physical damage)	Agricultural land (Production losses)
River and Coastal floods <i>Probabilistic</i> <i>Water extent and depth</i>	Impact model (Jonkman et al. 2008)	Impact model (Huizinga et al. 2017)	Exposure classification
Landslides <i>Deterministic</i> <i>Landslide hazard index</i>	Exposure classification	Exposure classification	
Agricultural drought <i>Deterministic</i> <i>Agricultural Stress Index</i>			Exposure classification
Heat stress <i>Probabilistic</i> <i>Wet-Bulb Globe Temperature index</i>	Exposure classification		
Air pollution <i>Deterministic</i> <i>PM2.5 concentration</i>	Exposure classification		
Tropical Cyclone <i>Probabilistic</i> <i>Maximum Sustained Wind Speed</i>	Exposure classification	Impact model (Eberenz et al., 2020)	Exposure classification

For this assessment, the vulnerability component is built over a set of global damage functions and quantitative impact classifications (thresholds table), specific for each hazard type. More details about the impact models for each combination are given in Annex 1. The poverty maps (presented in section 3.4) is used as proxy for socio-economic conditions to produce bivariate maps.

2.5 Risk

The risk estimate is calculated by combining hazard and exposure data in GIS. Areas with no hazard or no exposure are excluded from calculations. The unit of analysis is set to a resolution that matches that of the selected exposure layers. For the purposes of this analysis, the resolution is set to a common 90-metre grid. The impact model translates the physical intensity unit of a specific hazard into a damage factor (0 to 1), which is then multiplied by the exposure layer to obtain the impacted share over the total exposed value (*figure 7*).

Figure 7: illustrative example of spatial combination of hazard, exposure, and vulnerability components. The flood hazard layer (blue) describing water extent and depth (m) is overlaid to the exposure layer (orange) describing population count and built-up area. Where they match, there is an impact (pink) which is calculated as the product of the total exposure and the damage factor, which is driven by the impact model: depth-mortality function in the case of population (top-left box), depth-damage function in the case of built-up (bottom-right box).



When multiple probabilistic scenarios of hazard are available, the expected annual impact (EAI) is calculated by multiplying the impact from each event scenario with its exceedance probability ($1/RP_i - 1/RP_{i+1}$), and then summing up to one value (*figure 8*). The exceedance frequency curve shown in this figure highlights the relationship between the return period of each hazard and the estimated impact. The area below the curve represents the total annual damage considering all individual scenario probabilities.

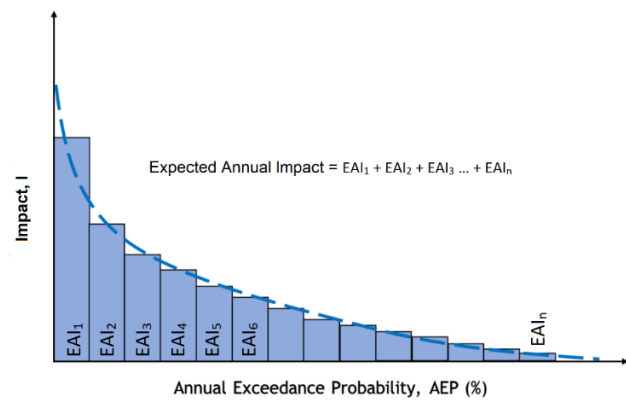
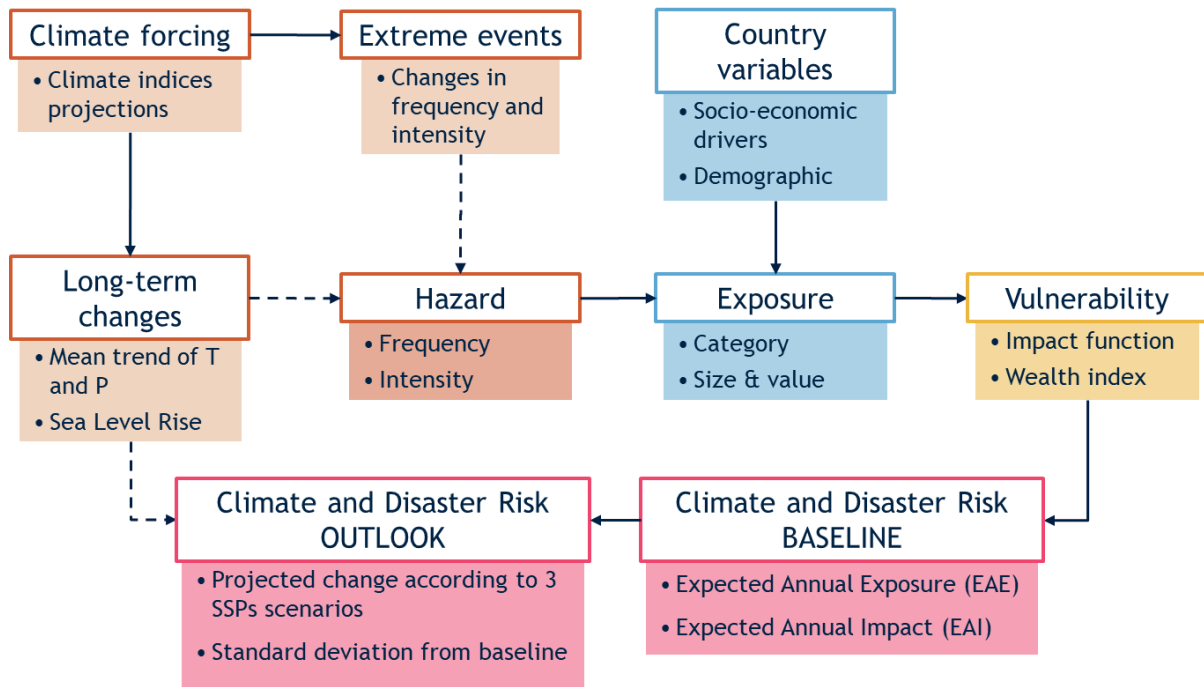


Figure 8: Computation of Annual Expected Impact of natural hazards in geospatial analytics

Figure 9 summarizes the workflow to calculate geographically disaggregated disaster risks.

Figure 9: Workflow to estimate geographically disaggregated disaster risks



3 Projecting risk into the future

The forward-looking analysis uses future climate projections to explore how environmental risks could develop spatially across Cambodia. The assessment of future impacts of climate change are based on comparisons of baseline conditions (which can be either observed or simulated) against future scenarios of climate variability. The long-term averages of climate variables serve as the baseline conditions. Changes in projected values against this baseline are then interpreted future climate anomalies and used to project forward-looking disaster risks. Given that specific unit of measurement varies across climate indices, all changes against the baseline are expressed in terms of Standard Deviation (SD) of the anomaly compared to historical variability (E3CI, 2020).

Data from climate models released under the IPCC Sixth Assessment Report (AR) framework ([IPCC 2021a](#)) are used to establish estimates of baseline and future projected climate anomalies. ARs are supported by coordinated climate modeling efforts referred to as Coupled Model Intercomparison Projects (CMIP). The analysis relies on CMIP6 data for modeling into the future, and takes into account three climate change scenarios, referred to as Shared Socioeconomic Pathways (SSPs) in CMIP6. These pathways cover the range of possible future scenarios of anthropogenic drivers of climate change by accounting for various future greenhouse gas emission trajectories, as well as a specific focus on carbon dioxide (CO₂) concentration trajectories ([IPCC 2021b](#)). The following scenarios are included in this analysis:

- SSP1/RCP2.6: low emissions declining to net zero after 2050
- SSP2/RCP4.5: intermediate emissions around current levels until 2050 before dropping off
- SSP5/RCP8.5: high emissions that roughly double from current levels by 2050

Each climate scenario predicts different spatial patterns, intensities, and frequencies of future natural hazards over 2041 to 2060. This information is aggregated at the level of individual states to identify units that are likely at risk of experiencing higher frequency and intensity of specific natural hazards. Key climate variables connected to the changing patterns of precipitation and temperature are summarized in *Table 2*.

Table 2: Climate variables underlying climate projections

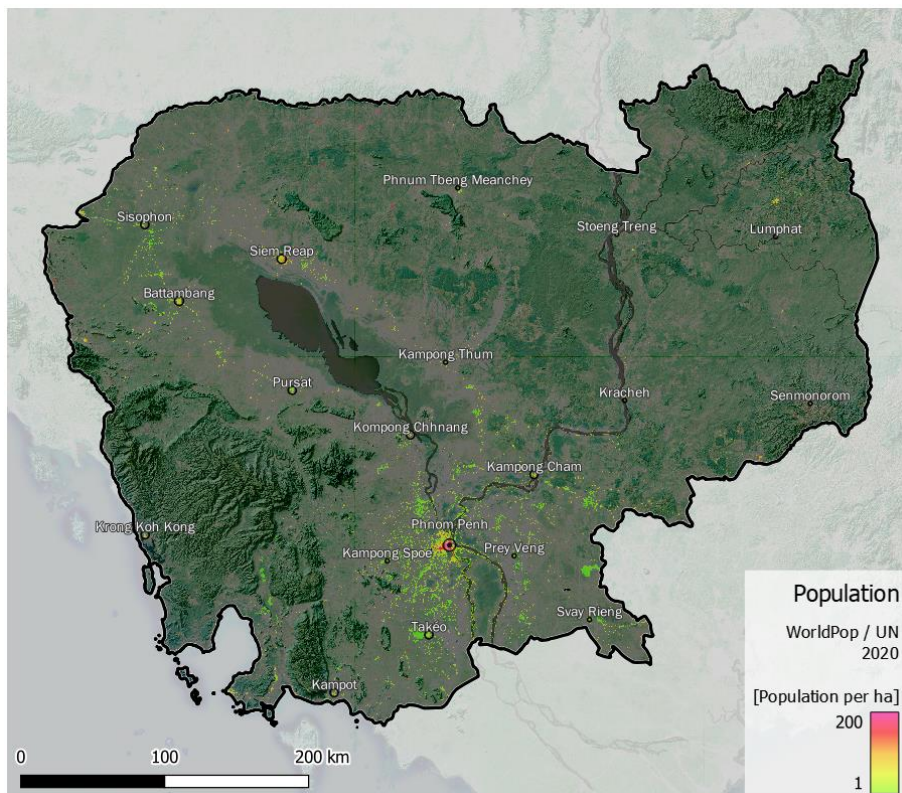
Hazard	Associated climate indices	Unit of measurement
Floods and Landslides	Rainfall > 10 mm	Days per year
	Consecutive wet days	Days per year
	Maximum 5-day precipitation	mm
	Extremely wet days	mm
	Sea Level Rise	m
Drought	Annual SPEI	Dimensionless
	Consecutive dry days	Days per year
Heat stress	WBGT Heat index	Days per year > 23 °C
		Days per year > 30 °C

4 Exposure data

4.1 Population

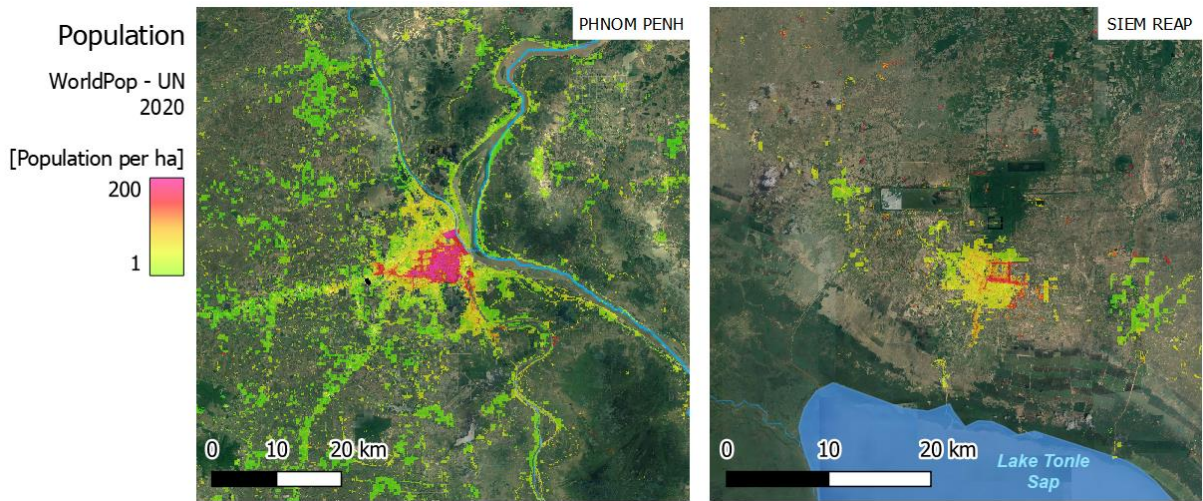
Whether an individual will be affected by a natural hazard depends on its location of residence. For localized extreme events such as floods or landslides, population data at administrative levels (for instance from censuses) do not offer the required granularity to measure their exposure. Therefore, high-resolution population data from [WorldPop 2020](#) population model ([Stevens et al., 2015](#)), with a 90-meter resolution, is used in the current analysis. *Figure 10* shows the distribution of the population across the country.

Figure 10: WorldPop 2020 population model for Cambodia – 100 m grid



Cambodia's population is estimated at around 16 million people (in WorldPop 2020), with bigger concentrations in central, southeast region, and around the capital of Phnom Penh, which accounts for about 2.2 million people. Another large concentration of population is located across the plains around Lake Tonle Sap and the Mekong River (*Figure 11*). In contrast and in line with Cambodia's population census, population densities are lower across the mountain regions in the northeast and southwest of the country, and around the densely forested areas in the central-north parts of Cambodia. The most populated are the districts pertaining to the urban areas of the capital Phnom Penh and surroundings, and Siemreap and Battambang in the North-West, while high population densities in the northern districts bordering Thailand are not matched by previous census values, and thus are likely due to WorldPop model overestimation. WorldPop estimates rely on population projections from the UN and distributes total population in proportion to built-up density obtained from remote sensing data. This can induce model errors, particularly in mountainous and forest environments, resulting in an overestimation of natural hazard risk in those areas. The aggregation of exposure and impacts at higher spatial resolution to an extent compensates for such biases, but residual errors cannot be ruled out suggesting careful interpretation of estimates is still warranted.

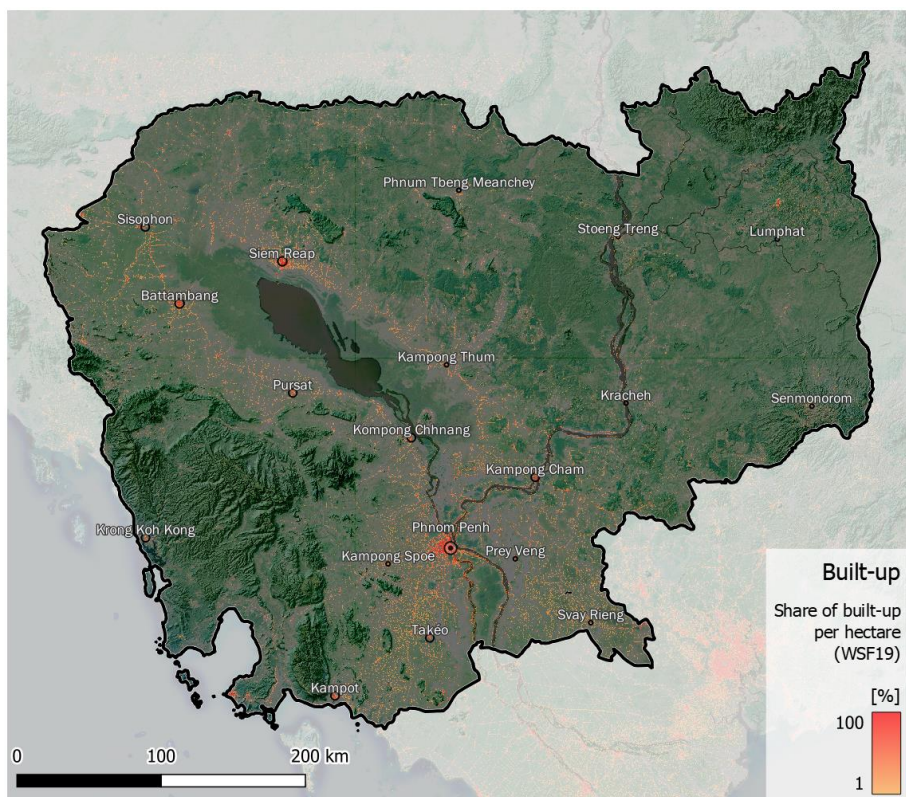
Figure 11: WorldPop 2020 population for the urban areas of Phnom Penh and Siem Reap, Cambodia



4.2 Built-up Assets

Built-up assets include homes, industrial complexes, road infrastructure, facilities, among other infrastructure. Data from [2019 World Settlement Footprint \(WSF\)](#) is used for this current analysis. This is a high-resolution (10m) remotely sensed dataset which indicates whether each cell is primarily built up. WSF data are resampled at 90-metre resolution to match the resolution of the WorldPop population data. The share of built-up land is then calculated for each cell (Figure 4). Similar to population distributions, built-up assets are most common around Cambodia's major cities, especially Phnom Penh, as well as over Tonlé Sap and Mekong plains.

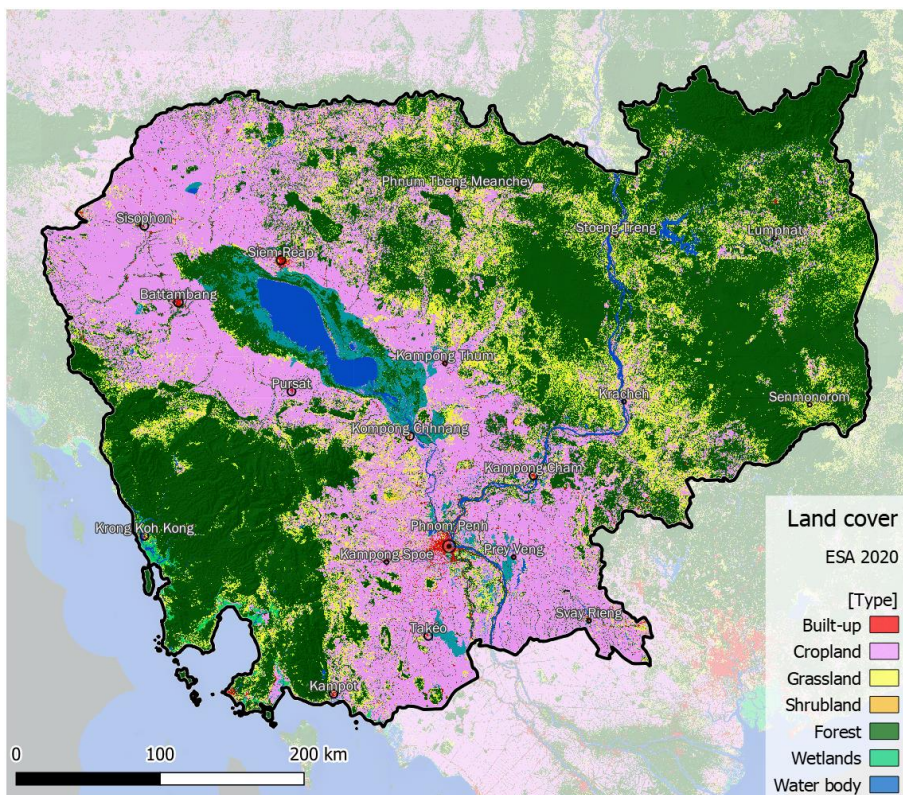
Figure 4: WSF 2019 distribution of built-up area across Cambodia



4.3 Land cover

The [2020 WorldCover](#) dataset at 10m resolution from the European Space Agency is used to identify agricultural land. The data are aggregated to 90m resolution and matched to the resolution of population model(*Figure 5*). Outside of Cambodia's major urban agglomerations, fertile cropland dominates in the centre and north-western parts of the country, with more sparsely vegetated, forested areas in the higher-elevation areas and upstream of the Mekong river.

Figure 5: ESA 2020 Land Cover across Cambodia



4.4 Administrative boundaries

Cambodia is divided into 24 provinces (ADM Level 1), which are referred to as '*khet*', and 1 special administrative unit of Phnom Penh ('*krong*'). ADM Level 1 units are subdivided into 202 districts (ADM Level 2) and further 1646 commune (ADM Level 3, municipalities).. The smallest level available (Level 3 - municipalities) is selected for aggregating the exposure and risk statistics.

5 Risk baseline: Mapping Hazard, Exposure and Vulnerability

The Expected Annual Impact or Expected Annual Exposure values are calculated following the combinations of available hazard, exposure and vulnerability models presented in *Table 1*.

5.1 Fluvial and coastal floods

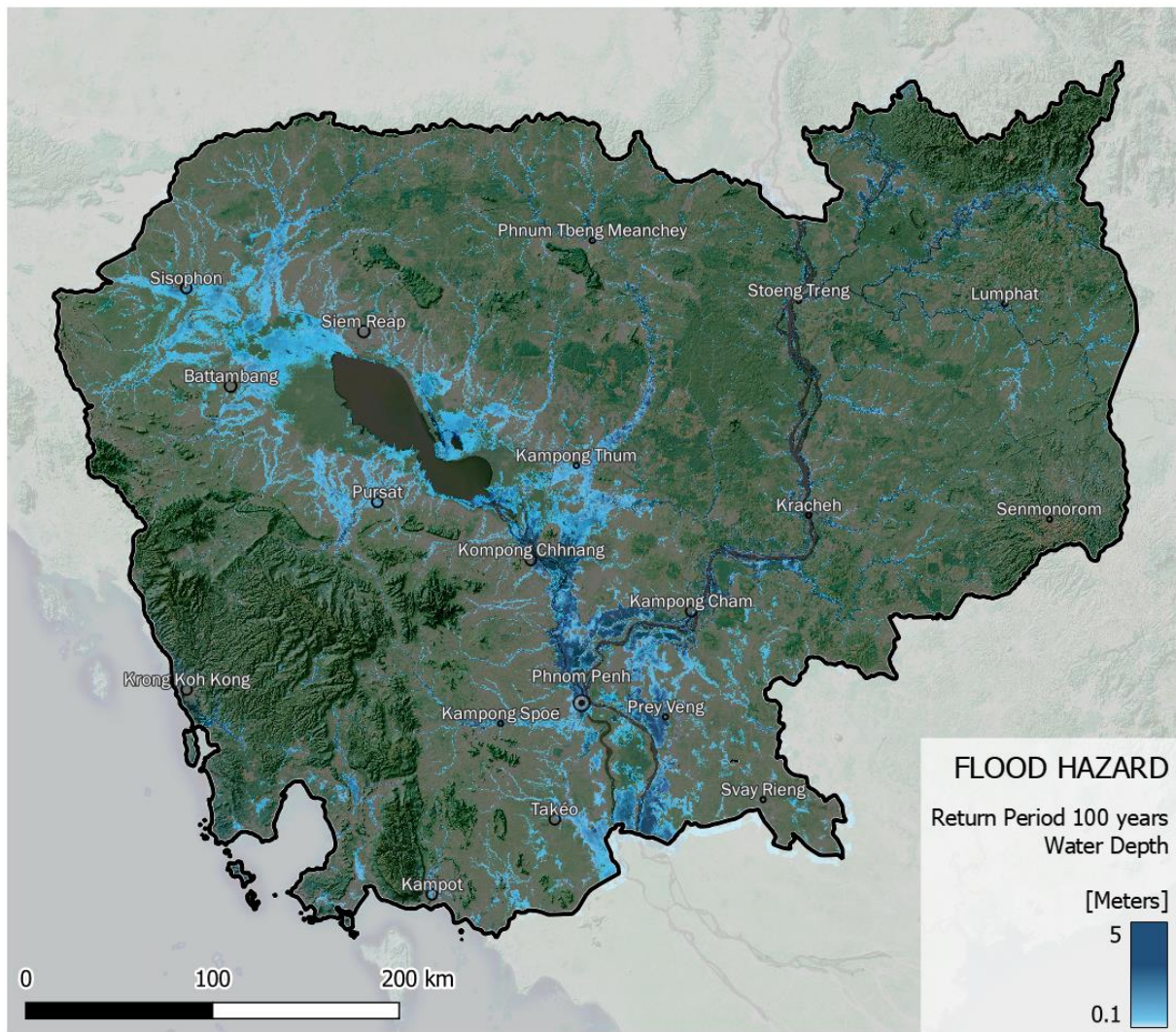
Flood is the most common and recurring disaster in Cambodia, linked closely with storms and tropical cyclones. It is exposed to significant hazard from inland fluvial (or riverine) floods, particularly along the Mekong and Tonle Sap floodplains, as well as flash floods due to extreme rainfall events, particularly during tropical cyclone events ([Chen et al., 2020](#)). Extreme rainfall can also trigger landslides across the country, particularly over the southern (Cardamom mountains) and north-eastern mountainous regions (Virachey National Park). The country has a south-west to north-east decreasing precipitation gradient, where annual precipitation is usually highest in the province of Koh Kong (3,200 mm/year) and lowest in Otdar Meancheay (1,300 mm/year). Rainfall is usually concentrated during the monsoon season, usually ranging from May to October and peaking around the months of June-July-August ([WBG 2021c](#)). The construction of dams, however, has been cited to affect flood levels in Cambodia in an insignificant way ([Phy et al., 2022](#)).

Major floods in Cambodia have been recorded at an average of 5 to 10 years frequency. One of the worst floods in recent history occurred in autumn of 2000, causing the Mekong River to hit a record water level of 11.2 meters. The event impacted 2.7 million people across Cambodia, damaged its agriculture sector and caused 374 fatalities. Roads and other critical infrastructure, including hospitals and public buildings, were badly damaged or partially destroyed ([ReliefWeb, 2000](#)). The total estimated reconstruction costs were estimated at around USD 156.7 million ([NCDM, 2000](#)). In 2011, another round of flooding inundated Cambodia, killing at least 250 people, including 83 children. Lowland regions along the Mekong River and mountain streams were worst affected. The total damage is estimated to be upwards of US\$ 500 million ([IFRC, 2011](#)).

While historically less relevant than riverine flooding, coastal flooding triggered by extreme sea levels and storm surges poses another major threat Cambodia. Sea levels are projected to rise between 44cm (RCP 2.6) to 78cm (RCP 8.5) by 2100 ([WBG, 2021](#)) and with an estimated 30,000 people potentially exposed to coastal flooding without adaptation by 2070–2100 under RCP 8.5 ([UK Met Office, 2014](#)). Similarly, another study by the World Bank Group showed that a 1m of sea level rise could results in flooding of around 80,000 people and cost 0.5 to 1% of Cambodia's GDP ([Dasgupta et al., 2007](#)).

Expected Annual Impact (EAI) of floods in this analysis is calculated using impact functions and data on population and built-up area. EAI values are then aggregated at ADM3 level for flood scenarios ranging from a return period of 5 years (that is, frequent flooding event with low magnitude) to 1,000 years (extreme flooding event with high magnitude). Similar impact functions for agriculture are not available, so cropland exposure is expressed for water stages over 0.5 meter. *Figure 6* captures the geographic distribution of flooding hazard for river and coastal flooding events with a 100-year return period, according to the Fathom and WRI global models. The Fathom dataset covers ten return periods, depicting how often flooding of a certain inundation depth occurs. Flood depths of up to 5 metres can be seen along the Tonle Sap and Mekong River systems, with floodplains around the cities of Phnom Penh, Kompong Chhnang, Kampong Cham, and Prey Veng. Lower floods depths are observed upstream and around the Lake Tonle Sap, to the central/north-western part of Cambodia. The capital city of Phnom Penh is considerably impacted by flooding hazard.

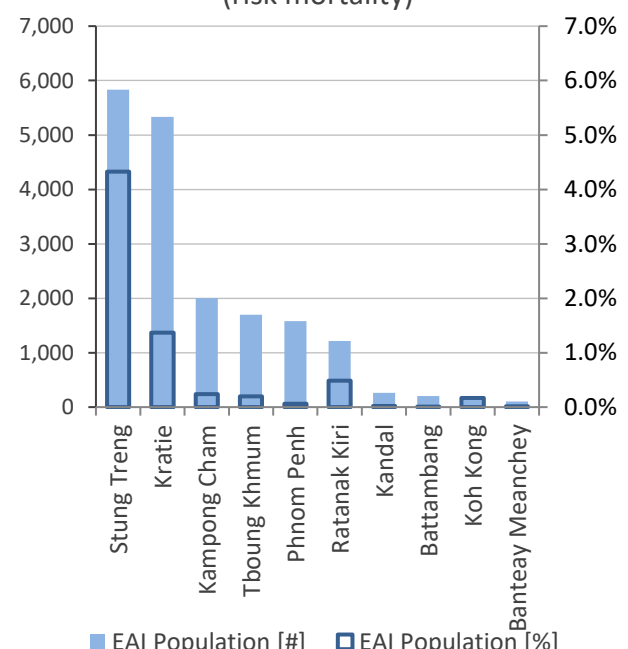
Figure 6: River flood hazard across Cambodia, Return Period 100 years

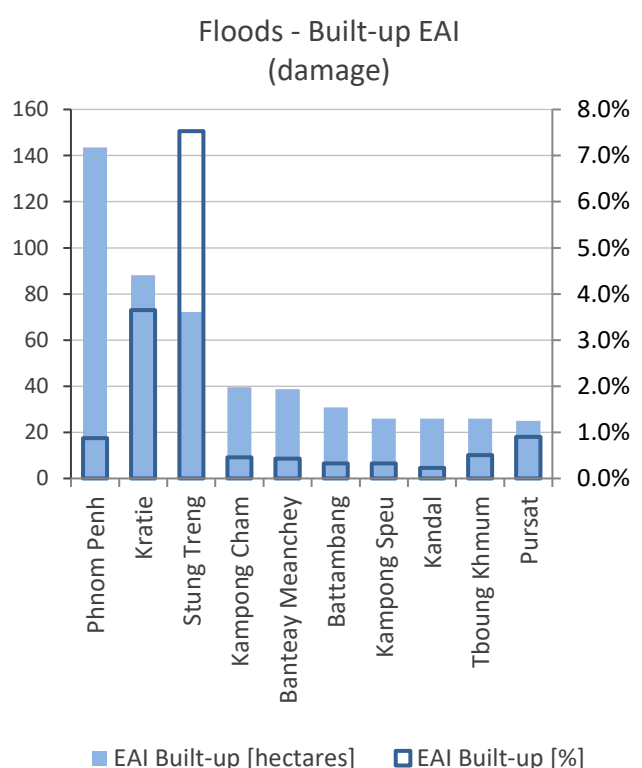
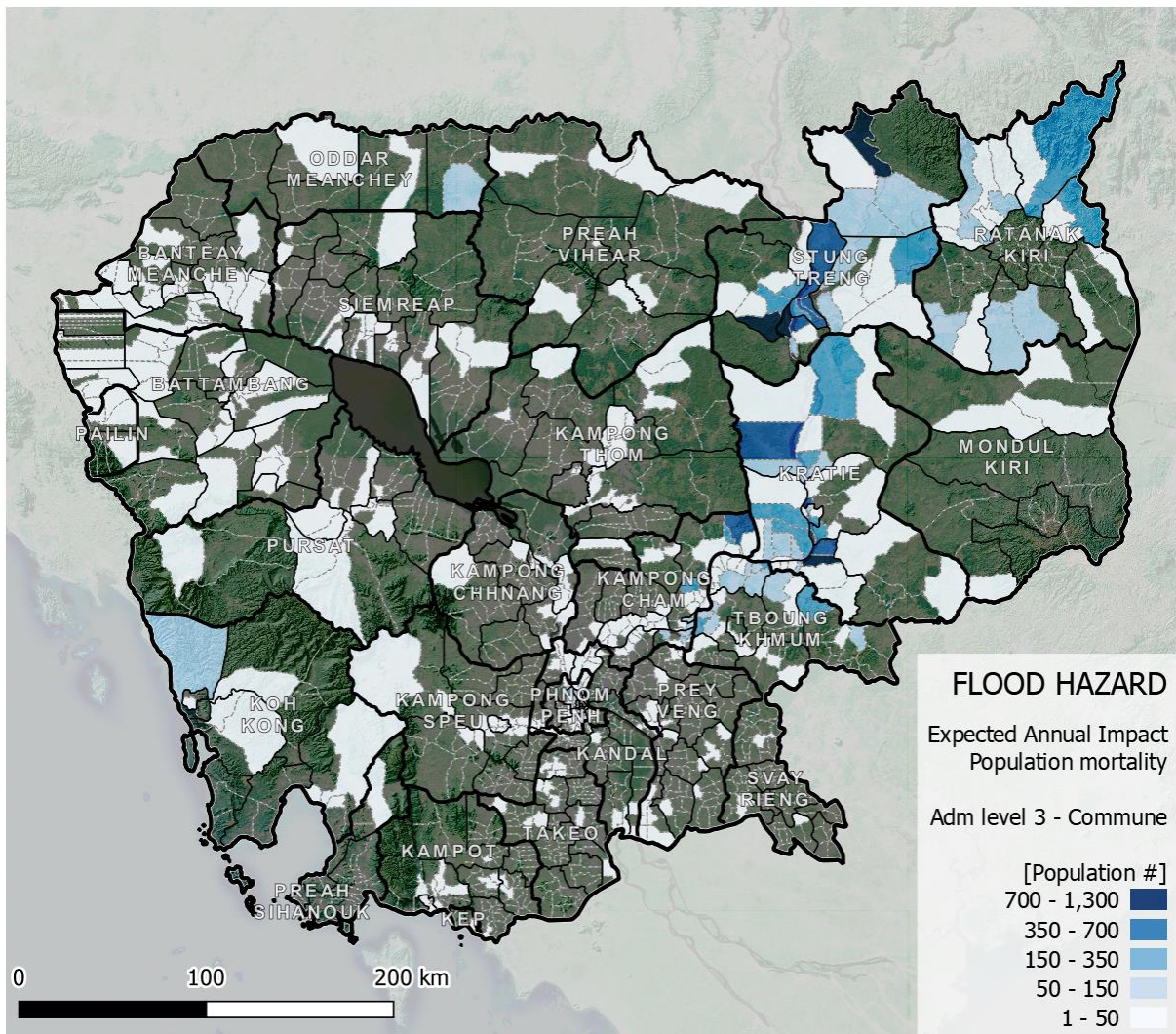


Population: the highest risk of mortality from flooding is largest along the valleys of Tonle Sap and Mekong rivers, especially in the densely populated capital of Phnom Penh and upstream Mekong basin (*Figure 7*). In Stung Treng, Kratie, Kampong Cham, Tboung Khmum, Ratanak Kiri, Kandal, Battambang, and Koh Kong, over 150 people are at risk of loss of life every year. The expected annual flood mortality is much lower in the less densely populated areas away from the river valleys, such as the regions of Svay Rieng, Mondul Kiri, Preah Sihanouk, and Kep. From the individual assessment of risks, we estimate that population mortality due to coastal flooding is minimal compared to riverine flooding, accounting for less than 1% of the flood risk and being mildly relevant in Koh Kong and Kampot.

Figure 7: Expected annual impact of riverine and coastal floods on population mortality

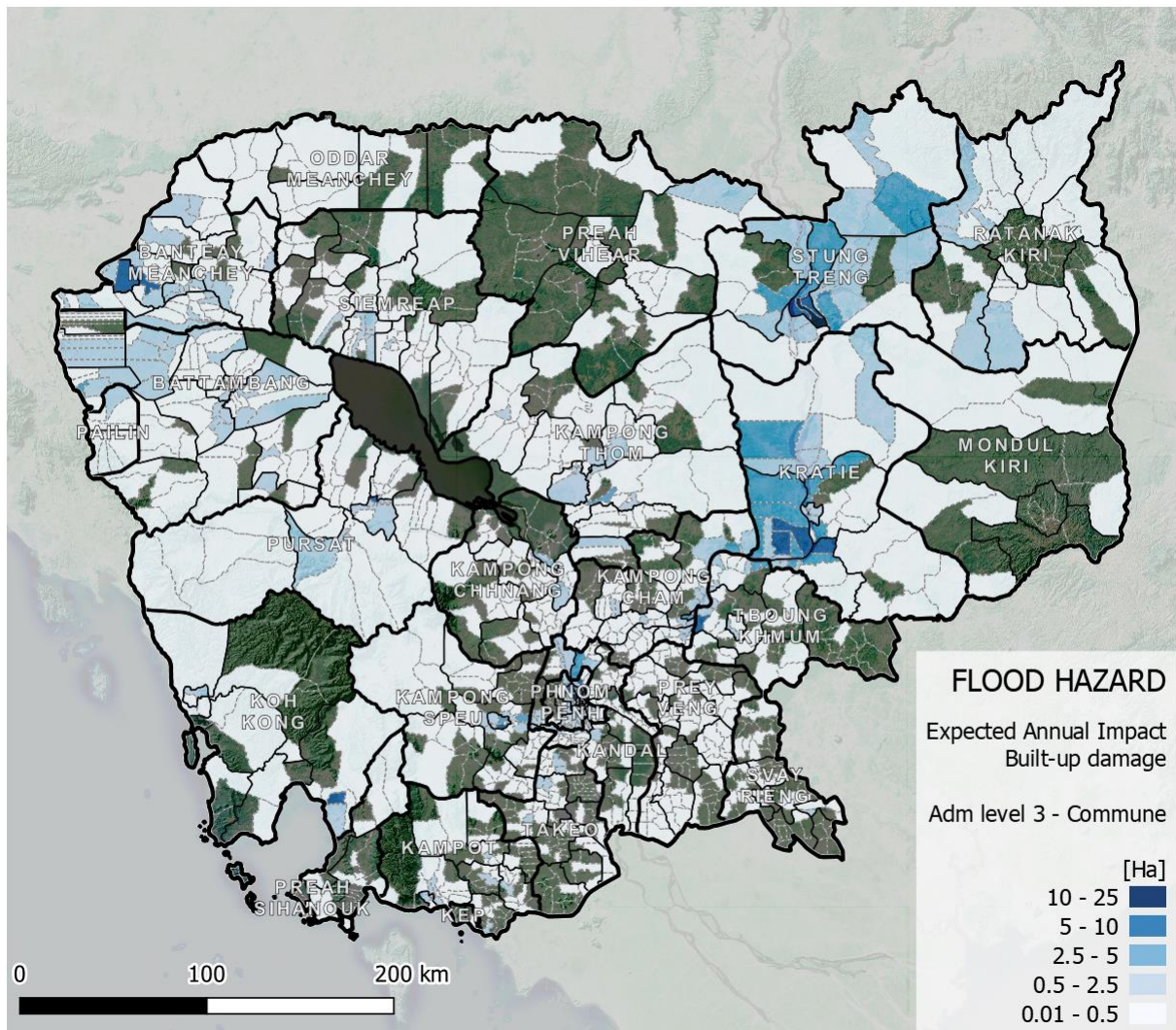
Floods - Population EAI (risk mortality)





Built-up: impact on the built-up environment is particularly high along the Mekong valley where large urban settlement areas in Cambodia are located (*Figure 8*). The capital Phnom Penh is at higher levels of flood risk, both in absolute but also in relative terms. Over thirty hectares of built-up including residential, industrial, and public infrastructure, are also at risk of damage in the provinces of Kratie, Kampong Cham, Stung Treng, and Banteay Meanchey.

Figure 8: Expected annual impact of riverine and coastal floods on built-up damage (ha of built-up destroyed)



Agriculture: Crop producing areas over the floodplains of the Mekong and Tonle Sap rivers have high exposure to riverine floods (Figure 9). The regions of Battambang, Banteay Meanchey, Kampong Thom, Kratie, Siemreap, Tboung Khmum, and Kampong Cham are likely to have more than 2% of their agricultural area exposed to floods over than 0.5m per year. In general, river flooding is much more relevant than coastal flooding, but agricultural exposed to coastal flooding is considerable in Kampot and Koh Kong provinces, with over 60 hectares of agricultural land expected to be exposed to coastal flooding every year.

Floods - Agriculture EAE
(exposure > 0.5m flood depth)

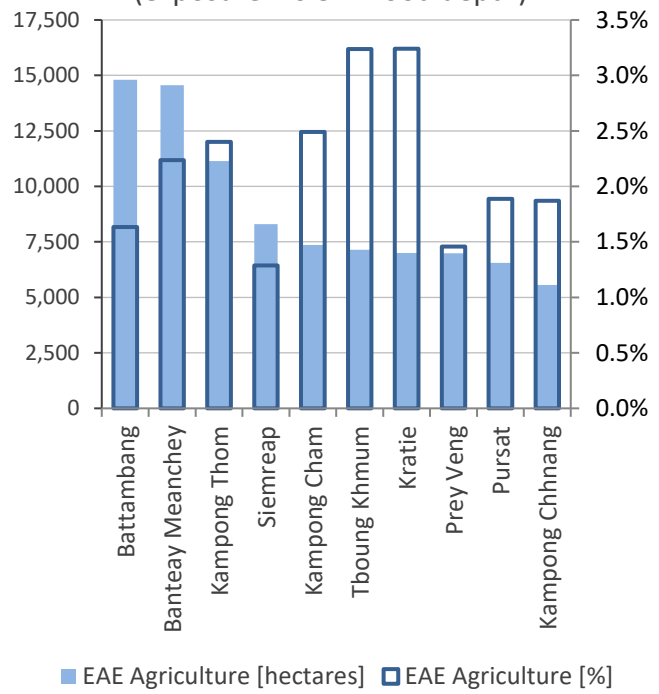


Figure 9: Expected annual exposure of agricultural land to riverine and coastal floods for water depth above 0.5 meters

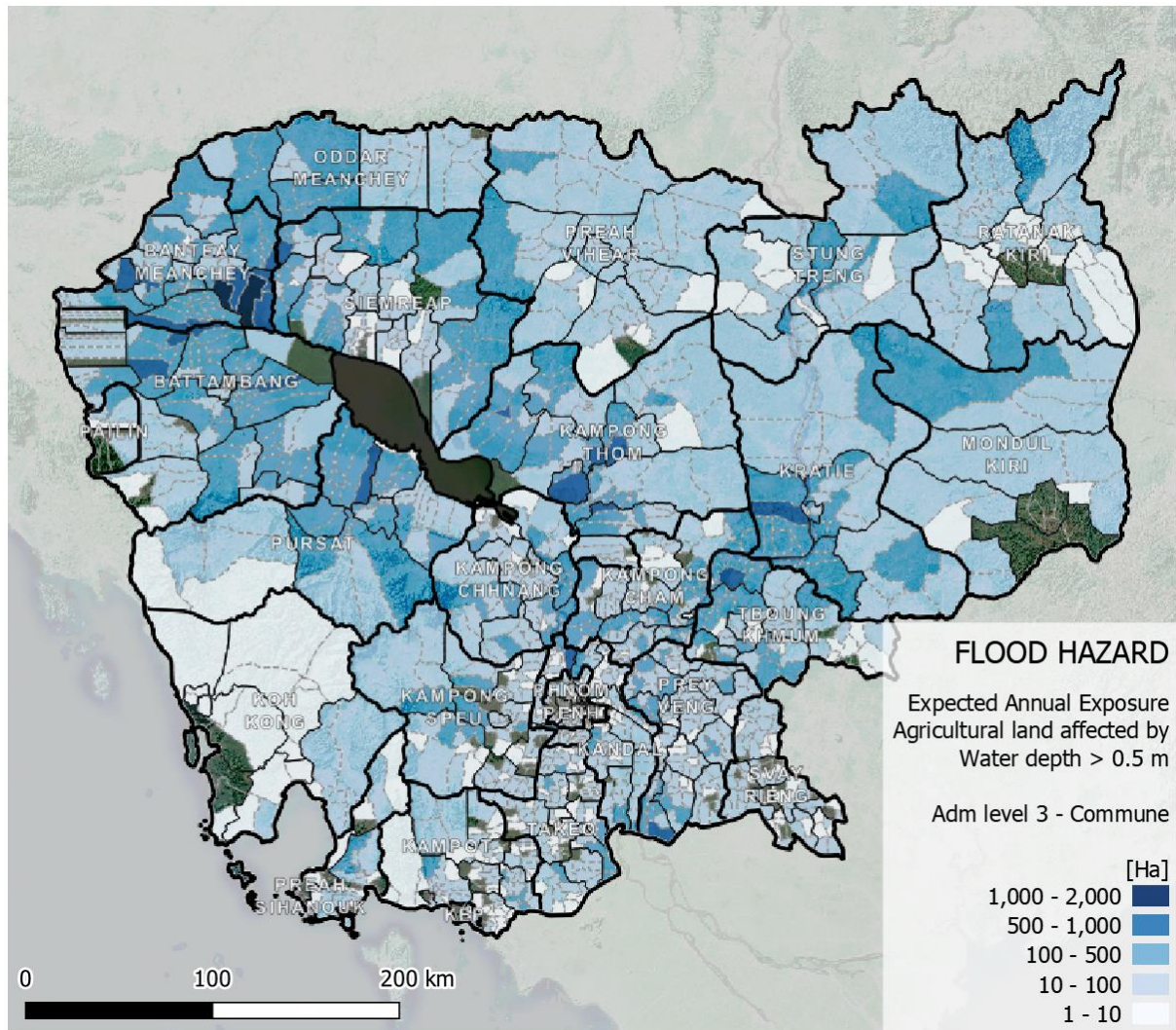


Table 3 presents the calculation of total EAI for population and built-up exposure categories, as explained in section 2.4.

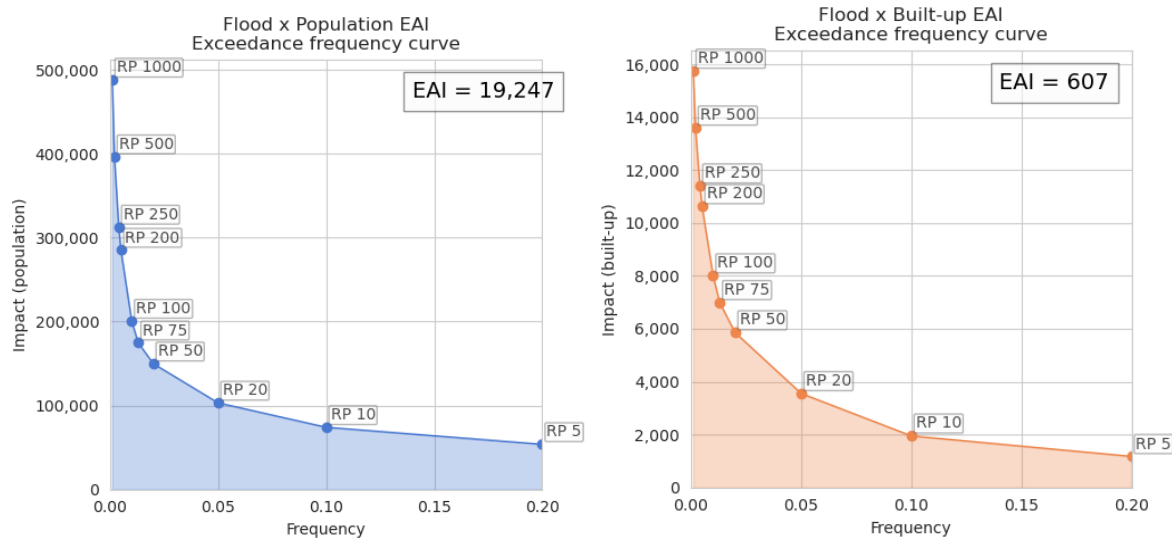
Table 3: Expected Annual Impact from probabilistic analysis of flood risk over population and built-up (10 Return Periods).

Return Period [years]	Probability	Population impact [#]	Population EAI [#]	Built-up impact [ha]	Built-up EAI [ha]
5	0.2	53,827	2,691	1,175	59
10	0.1	74,124	5,559	1,950	146
20	0.05	103,218	4,129	3,555	142
50	0.02	149,891	2,748	5,856	107
75	0.013	174,916	875	6,995	35
100	0.01	200,795	837	8,006	33
200	0.005	285,418	856	10,622	32
250	0.004	312,984	469	11,405	17
500	0.002	396,756	595	13,592	20
1,000	0.001	488,165	488	15,742	16
Total		19,247		607	

The charts in *Figure 10* show the Exceedance Frequency Curve for river floods over population (left) and built-up (right). The EAI for each category is calculated as the area below the curve: according to the models, every year floods are estimated to put, on average, over 19,247 people at risk of mortality from high floodwater levels, and to trigger a loss of built-up over 600 ha. Note that both estimates are cumulative over the total value, e.g. 2 ha of built-up suffering 50% damage are summed up as 1 ha of built-up suffering complete damage.

According to this data, large impacts over exposed categories are expected from frequent flood events of moderate magnitude (RP 5 and 10 years). This seems consistent with the trend highlighted by the recent disaster records.

Figure 10: Exceedance frequency curves for flood hazard over population (left) and built-up (right).



5.2 Agricultural drought

In addition to flooding, variability in rainfall causes frequent drought episodes in Cambodia. The main cause of droughts in Cambodia is meteorological, primarily due to precipitation variability induced by El Niño that is often associated with moderate to severe droughts in Cambodia ([Lyon, B., 2004](#)). Currently, Cambodia faces an annual median probability of severe meteorological drought of around 4% ([CCKP, 2021](#)).

Cambodia experienced a severe drought in 2022, and in 2015 to 2017. These episodes caused crop damages and loss of livelihoods, primarily among poor subsistent farmers and small land holders ([Hill, 2016](#)). Overall, 18 out of 25 provinces were severely affected by these episodes, impacting over 2.5 million people ([CEDMHA. 2017](#)). Droughts also indirectly impact welfare by increasing the competition for water resources magnified by the large share of country's population that continues to rely on natural resources for domestic consumption ([UNDP, 2011](#)).

The current analysis uses drought probability estimates at from FAO's Agricultural Stress Index (ASI). The index measures the share of agricultural land (cropland and pasture combined) at a 1km resolution that is affected by drought annually between 1984 and 2022.

Regional drought impacts: Figure 11 and 12 shows . the fraction of years over a 34-year period (1984 to 2022) during which at least 30% of cropland within a grid was exposed to agricultural drought stress. A few districts, mostly located in mountainous areas in the southwest and northeast regions, have rarely experienced drought in the past. In contrast, droughts affected the region around Phnom Penh, Svay Rieng, Prey Veng, and Pailin, once every five to six years on average. Over 30% of cropland in these areas frequently experience drought stress, potentially leading upto crop failures and food insecurity.

Droughts - Frequency affecting at least 30% of cropland over the past 37 years

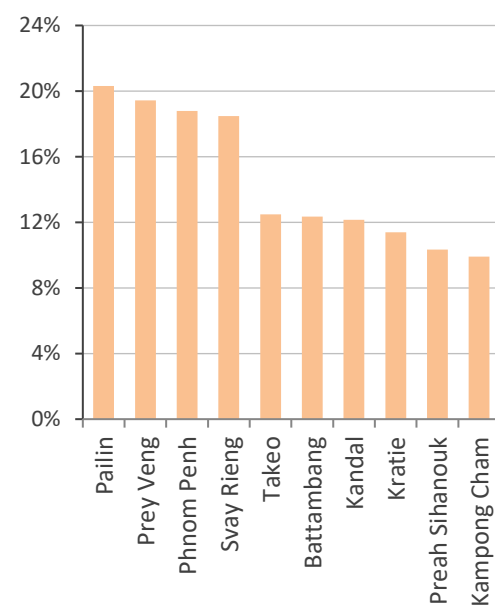


Figure 11: Frequency of drought hazard affecting at least 30% of crop across Cambodia during the primary cropping season (April-October)

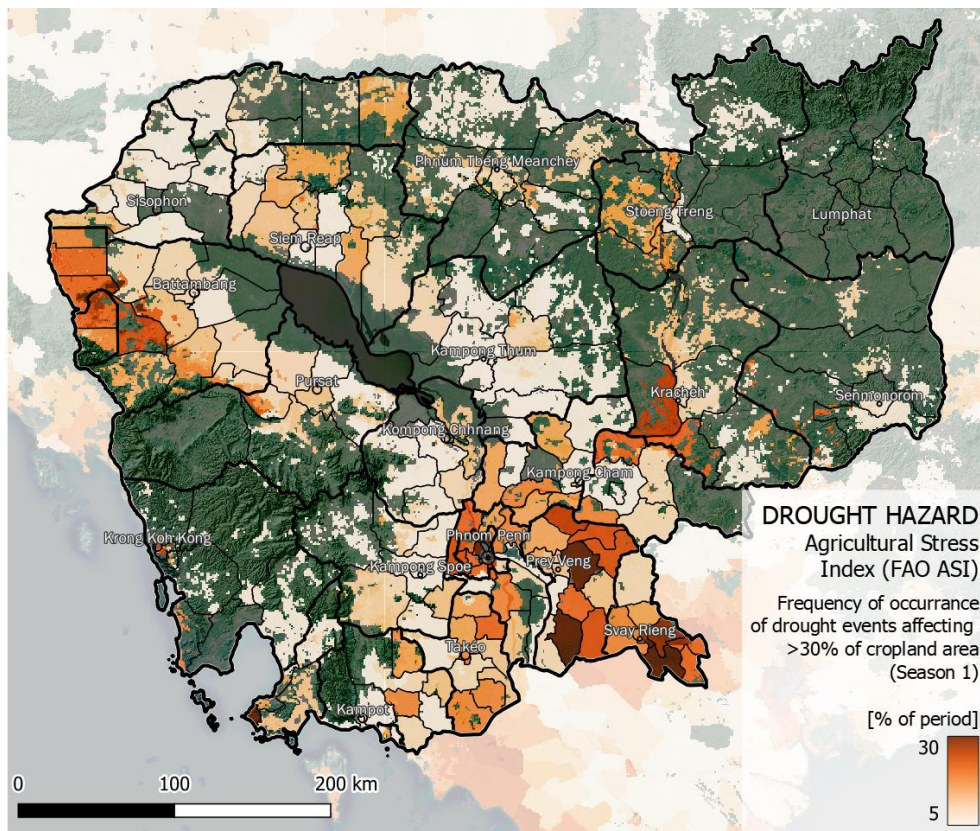
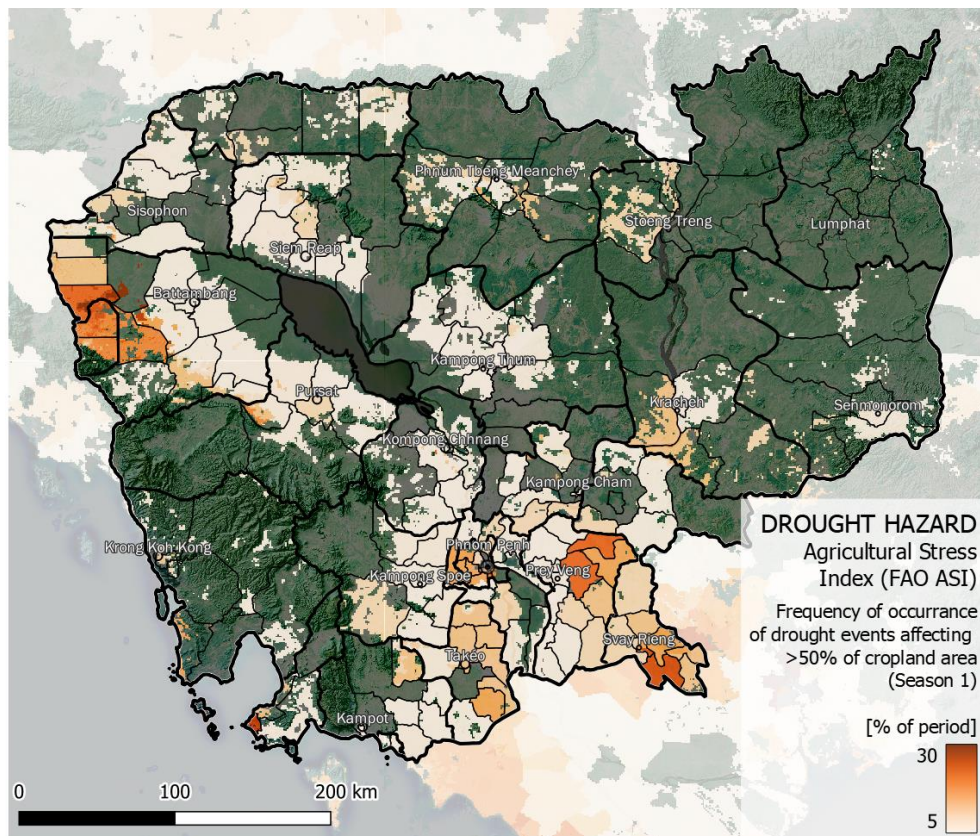


Figure 12: Frequency of drought hazard affecting at least 50% of crop across Cambodia during the primary cropping season (April-October)



Drought impacts on crops: Maize and rice are the most important crops in terms of cultivated area (ha) and production (tonnes) in Cambodia (*Table 4*). In terms of livestock, Cambodia's main commodity is pork, followed by chicken, cattle, and ducks. *Figure 13* and *14* show the historical exposure to drought according to FAO-GAEZ's 2015 crop distribution and FAO's ASI mean value over the period 1984-2022. The exposure to levels of severity of drought are almost equally distributed across main crops in Cambodia (exposure to drought for rice crops is slightly numerically higher than maize at all levels of severity). Similarly, severity of drought impacts are equally distribution across different types of livestock.

Table 4: main crop types extension in hectares for the period 2010-2020 (FAOSTAT)

CROP	Area harvested [million ha]											
	2010	2011	2012	2013	2014	2015	2016	2017	2018	2019	2020	MEAN
Maize	0.21	0.17	0.22	0.21	0.12	0.08	0.13	0.15	0.24	0.17	0.18	0.17
Rice	2.78	2.97	3.01	2.96	2.86	2.80	2.89	2.97	3.04	2.96	2.92	2.92

Figure 13: Agricultural stress index for droughts affecting over 30% and 50% agricultural land, primary season - Main crops

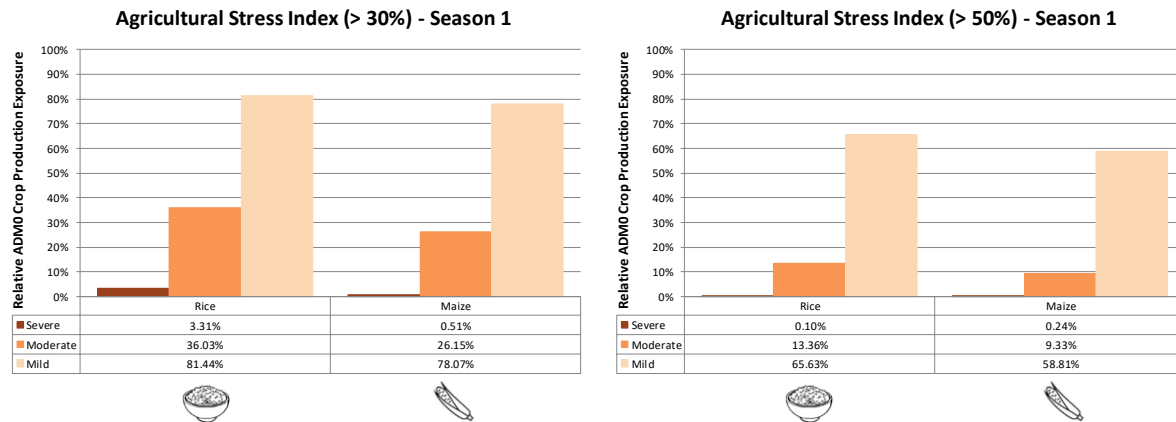


Figure 14: Agricultural stress index for droughts affecting over 30% and 50% agricultural land, primary season - Main livestock exposed

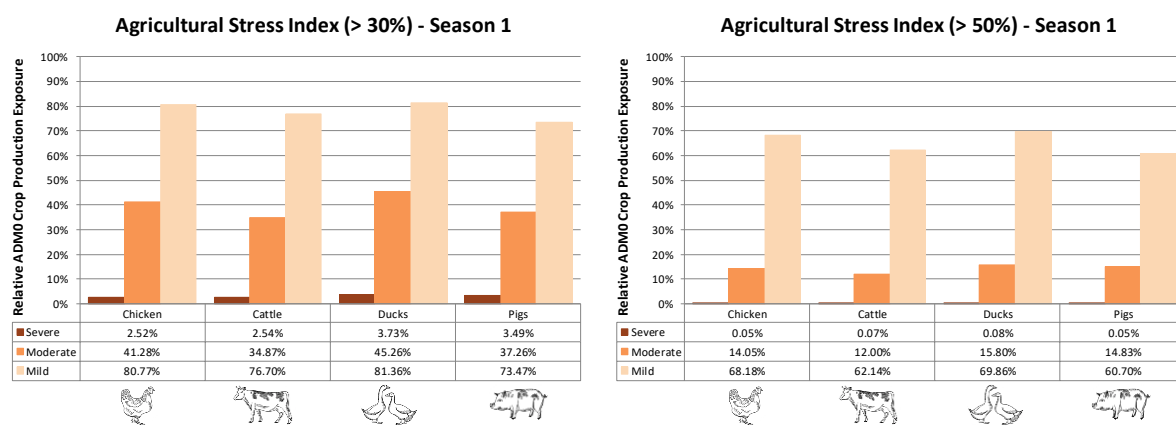
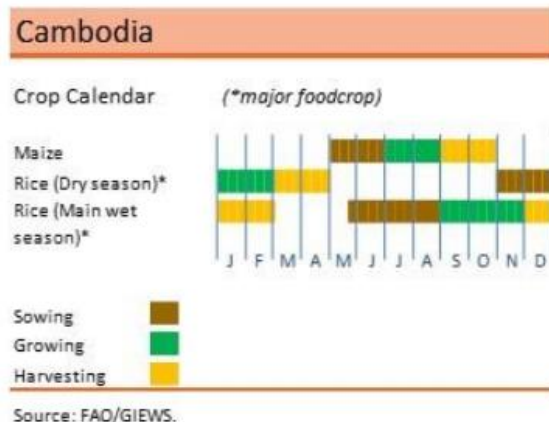


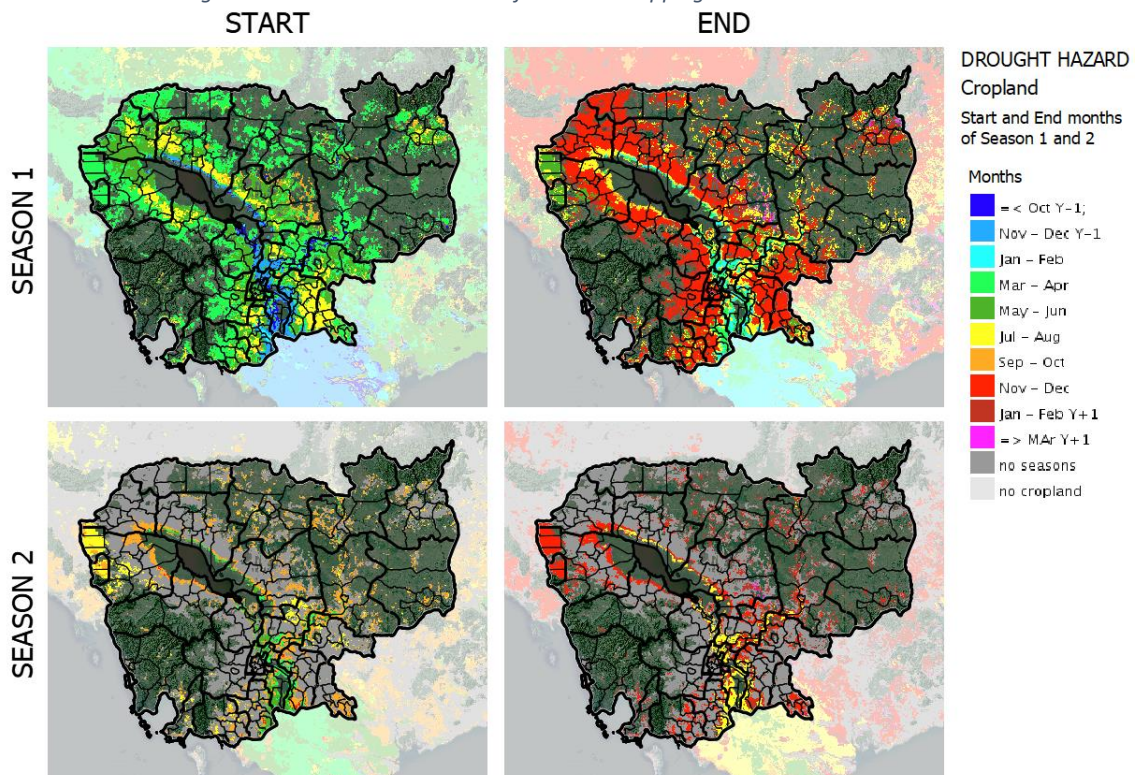
Figure 15: Crop calendar for most common important crops



the Mekong and Tonle Sap rivers and their associated floodplains. The annual yield of all fisheries, including fish and other aquatic organisms, is estimated to be around 750,000 tonnes, and aquaculture alone contributes to around 15-20% of this total ([FiA, 2014](#)).

Figure 15 shows the calendar phases of the major food crops for the country. Most of the production cycle occurs between May and November. Most of the agricultural activity in Cambodia is located along the Mekong and Tonle Sap river valleys (Figure 16). Cropping season starts in April-May and ends around October and November. Other than crops and livestock, aquaculture and fishery production are important components of the agricultural sector in Cambodia. Fisheries are mostly located in the Tonle Sap Lake, but also along

Figure 16: Start and end months of the main cropping season across Cambodia

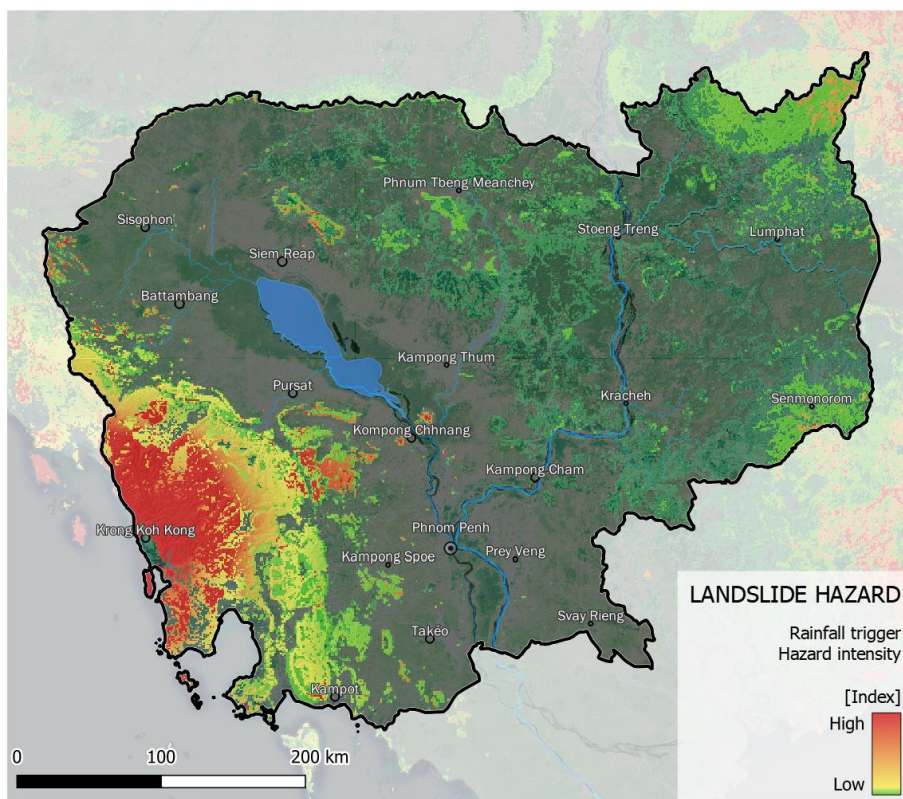


5.3 Landslides

Extreme rainfall can temporarily alter water pressure within the soil causing soil slope to exceed its stability point, inducing landslides or mudslides. Prolonged heavy rainfall, combined with porous soil and a high soil moisture content, are primary causes of landslides, particularly in the southwestern part of the country. However, there are no systematic databases of past landslide occurrences available in Cambodia. This makes it difficult to predict the occurrence and impact of such events. On October 2022, heavy rainfall in Cambodia and Vietnam, triggered floods and a number of landslides ([ECHO, 2022](#)). The combination of events impacted 165,000 people in Cambodia, 5,000 evacuations, damages to 33,500 and at least 15 fatalities ([ECHO, 2022](#)). Land use change and deforestation can magnify the intensity of landslides. Indeed, forest cover in Cambodia has declined dramatically in the last few decades, as agriculture has expanded: according to [FAO \(2010\)](#), agricultural land expanded from 26% to 31% of the total land area between 1997 and 2007.

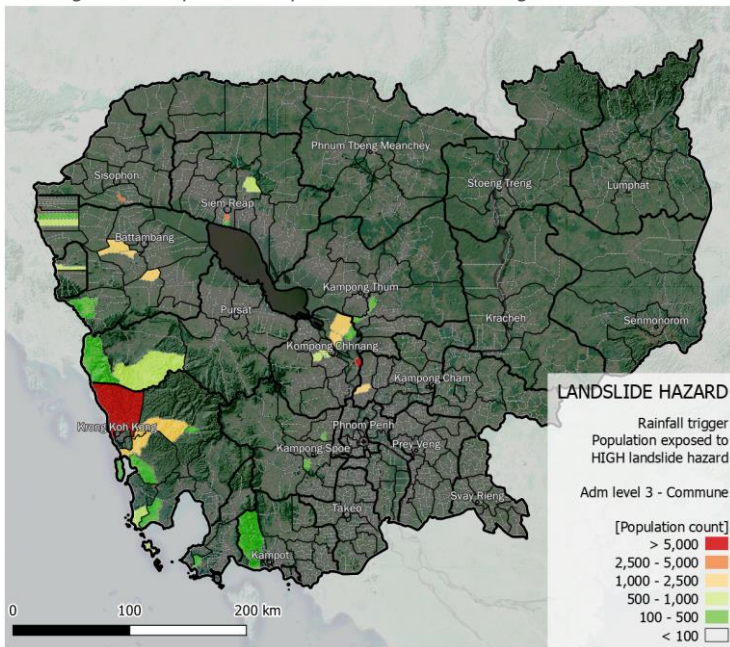
Landslide probability in this analysis is derived from World Bank-ARUP landslide hazard index available at 1km resolution (*Figure 17*). As there are no tailored impact functions available for landslides, impact estimate calculations rely on population, built-up asset, and agricultural exposure for this hazard. *Figure 18* shows the district-level population exposure to landslides, while *Figure 19* shows exposure of built-up assets for this administrative level.

Figure 17: Rainfall-triggered Landslide Hazard Index for Cambodia at 1km resolution



Both population and built-up exposure to landslide hazards are concentrated in same set of states: Battambang, Koh Kong, Kampong Chhnang, and Siemreap; and, to an extent, Banteay Meanchey, Kampong Chnam and Pursat. Over 35,000 people live exposed to significant rainfall-triggered landslide hazard in Battambang, and over 100 hectares of built-up assets are exposed to damage in Koh Kong, Battambang and Kampong. In total, about 80 thousand Cambodians are exposed to significant health and livelihood risks due to landslides.

Figure 18: Population exposure to medium or high landslide risk



Landslides - Population EAE
(exposure to high hazard)

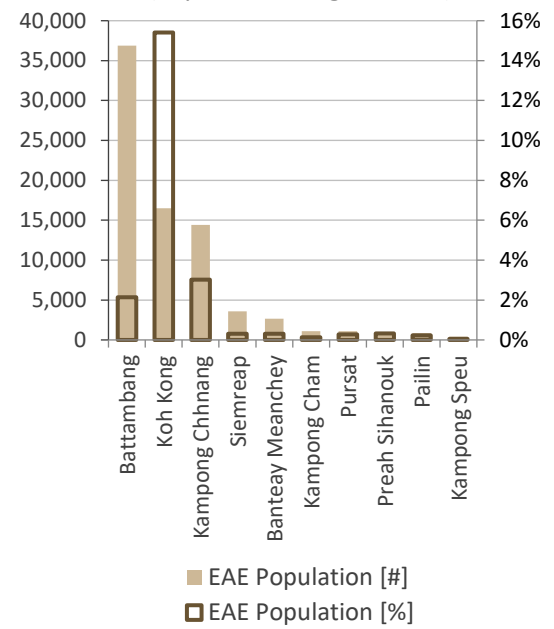
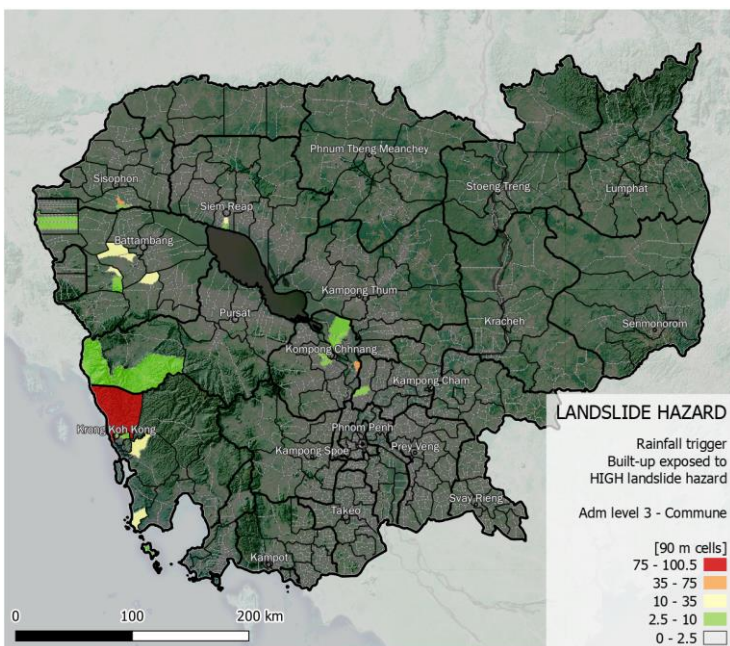
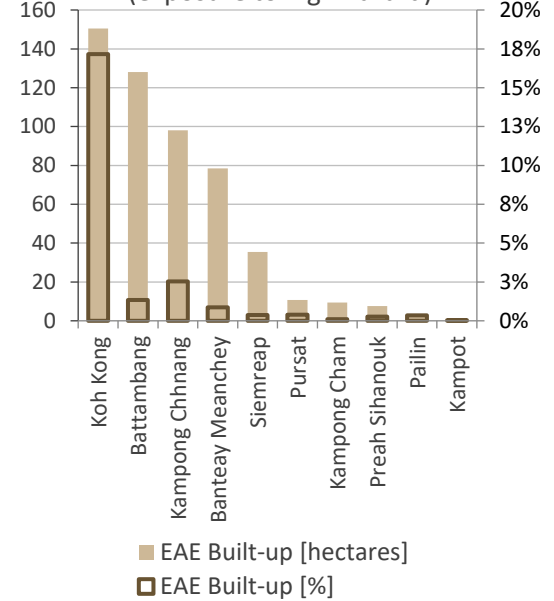


Figure 19: Built-up asset exposure to medium or high landslide risk



Landslides - Built-up EAE
(exposure to high hazard)



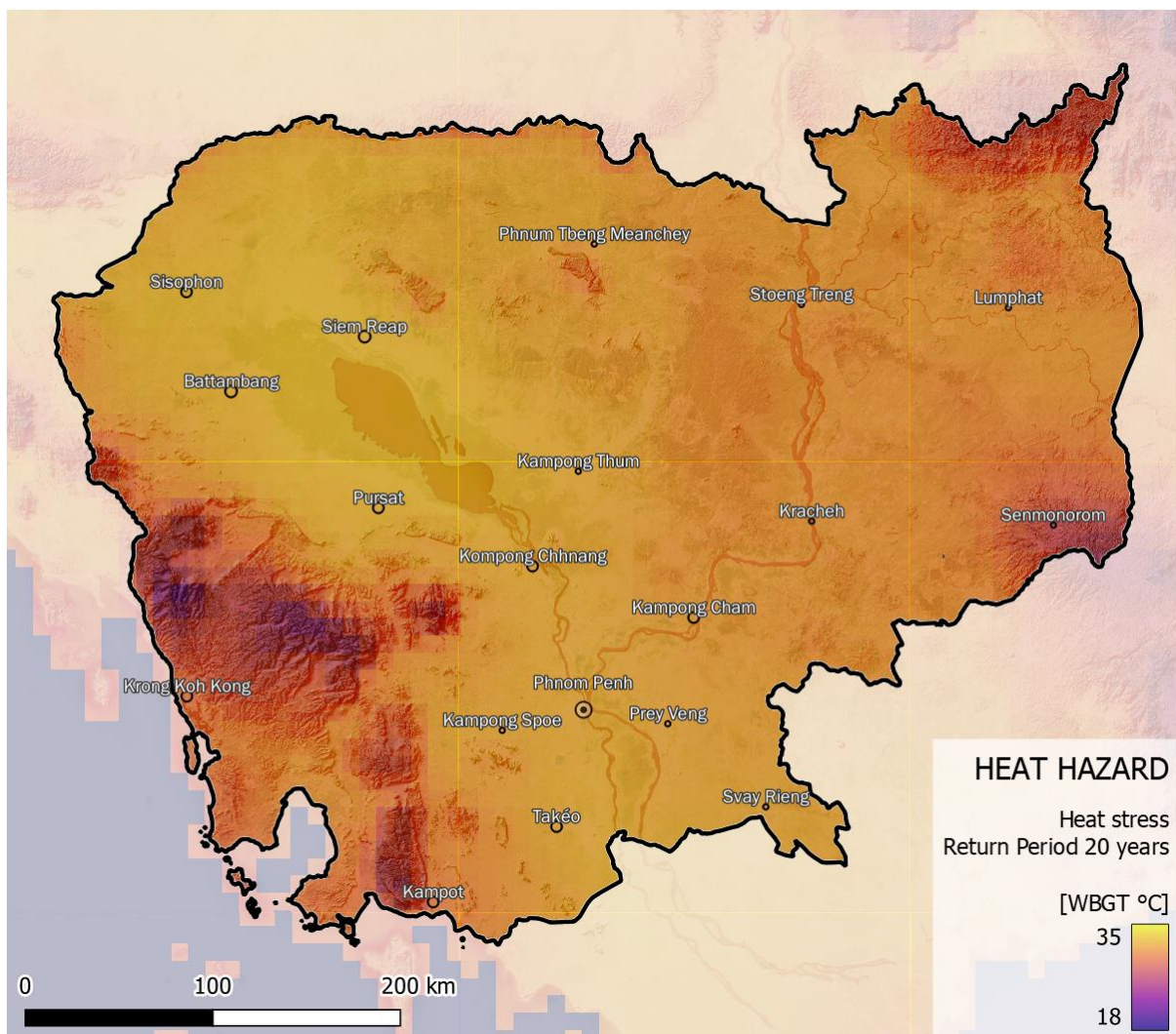
5.4 Heat stress

Human health is highly sensitive to the thermal environment (WHO 2008). Extreme heat events lead to heat stress and can increase morbidity and mortality (Garcia-Herrera *et al* 2010, NOAA Watch 2014) as well as losses of work productivity (Kjellstrom *et al* 2009, Singh *et al* 2015). Heat waves can cause long-term impairment to learning capacity and reduce labour productivity and incomes (Goodman *et al.* 2018).. Heat discomfort increases when hot temperatures are associated with high humidity (Coffel *et al.* 2018). Not everyone reacts to the heat stresses in the same way, as individual responses are conditional on their medical condition, level of fitness, body weight, age, and economic situation (National Institute for Occupational Safety and Health, 2016). The current analysis focuses on the impact of heatwaves on health and productivity.

The compounded effect of heat waves and urban heat islands represent a major threat to human health in Cambodia, particularly for laborers that work outdoor and in urban environments ([WBG 2021](#)). Cambodia is exposed to one of the highest annual average temperatures in the world, with an estimated 64 days per year of maximum daily temperature over 35°C ([CCKP, 2021](#)). The intensity of extreme heat hazard is higher over the central plains of Mekong and Tonle Sap rivers, which have the highest density of population and agriculture (see *Figure 20*). Over 550 million children in Cambodia (or 1 every four children in the country) are already currently exposed to high heatwave frequency ([UNICEF, 2022](#)). Extreme heat related mortality is likely to further exacerbate due to climate change making Cambodia one of the top 23 countries with critical exposure to extreme heat. A report from the World Health Organization ([WHO, 2016](#)) estimated that under a high emissions scenario, heat-related deaths in Cambodia for the elderly (65+ years) are projected to increase to about 56 deaths per 100,000 people by 2080 compared to the estimated baseline of about 4 death per 100,000 annually between 1961 and 1990. concludes,

In this report, heatwave probability is measured by the maximum daily Wet Bulb Globe Temperature (WBGT, in °C). The WBGT combines temperature and humidity, both critical components in determining heat stress.

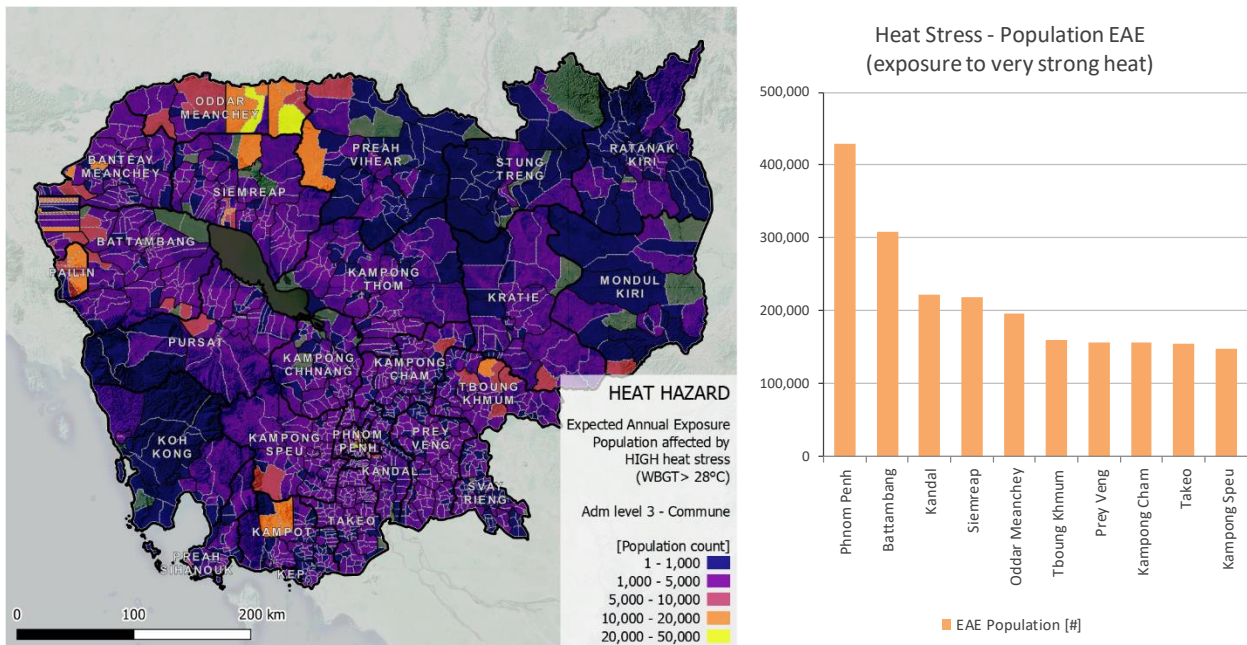
Figure 20: Heat stress across Cambodia for a heat event with 20-year return period



Three return periods of heat events are included in the analysis: once in 5, 20, and 100 years. *Figure 29* represents modelled maximum heat for the 20 year return period scenario. Wet bulb globe temperatures around 35 °C are common during heat stress episodes across Mekong and Tonle Sap valleys, implying that a large share of the country's population is exposed to heat stress.

Population: *Figure 21* shows the annual expected population exposure combining the three hazard scenarios. Thousands of Cambodians, especially those in dense urban centres (Phnom Penh, Battambang, Ta Khmau, Siem Reap, and Samraong) face exposure to very strong heatwaves at an annual basis, with severe health and economic implications.

Figure 21: Annual population exposure to high heat stress across Cambodia.

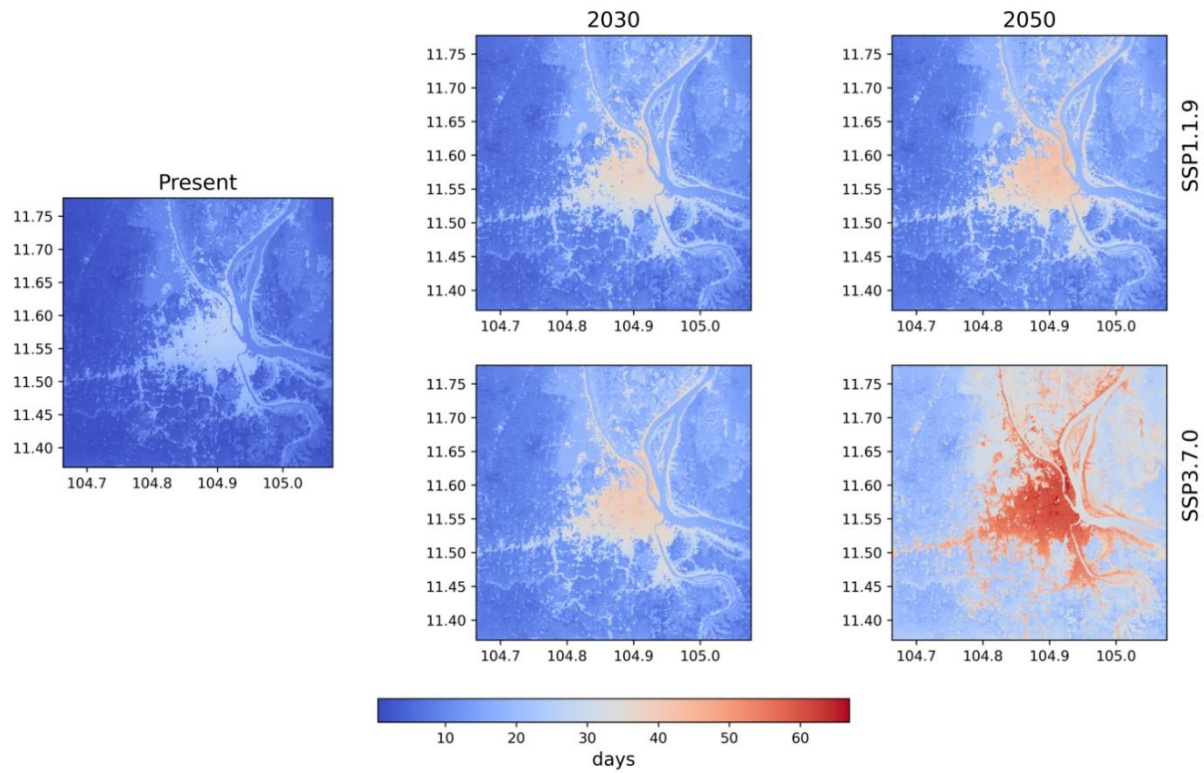


A recent study by the world bank (Souverijns et al., 2022¹) shows that in the metropolitan area of Phnom Penh, climate change has already caused a temperature increase by more than 1°C relative to pre-industrial values.

Figure 30: annual number of heatwave days for Phnom Penh at present, and towards the future (2030 and 2050) under low- and high-emission climate change scenarios (SSP1-1.9 and SSP3-7.0). At present, 25 heatwave days per year are observed in

¹ Niels Souverijns, Filip Lefebvre, Sacha Takacs (VITO) 2022. Urban heat: Piloting rapid assessment methodology: Technical annex. Study accomplished under the authority of the The World Bank Group. Contract 7206682 RMA/LUCI/21119. 9 December 2022. Distribution: Restricted

the city, while in future projections (for instance, 2050) this escalates to 40 days under SSP1-1.9 scenario and 60 under SSP3-7.0 scenario.

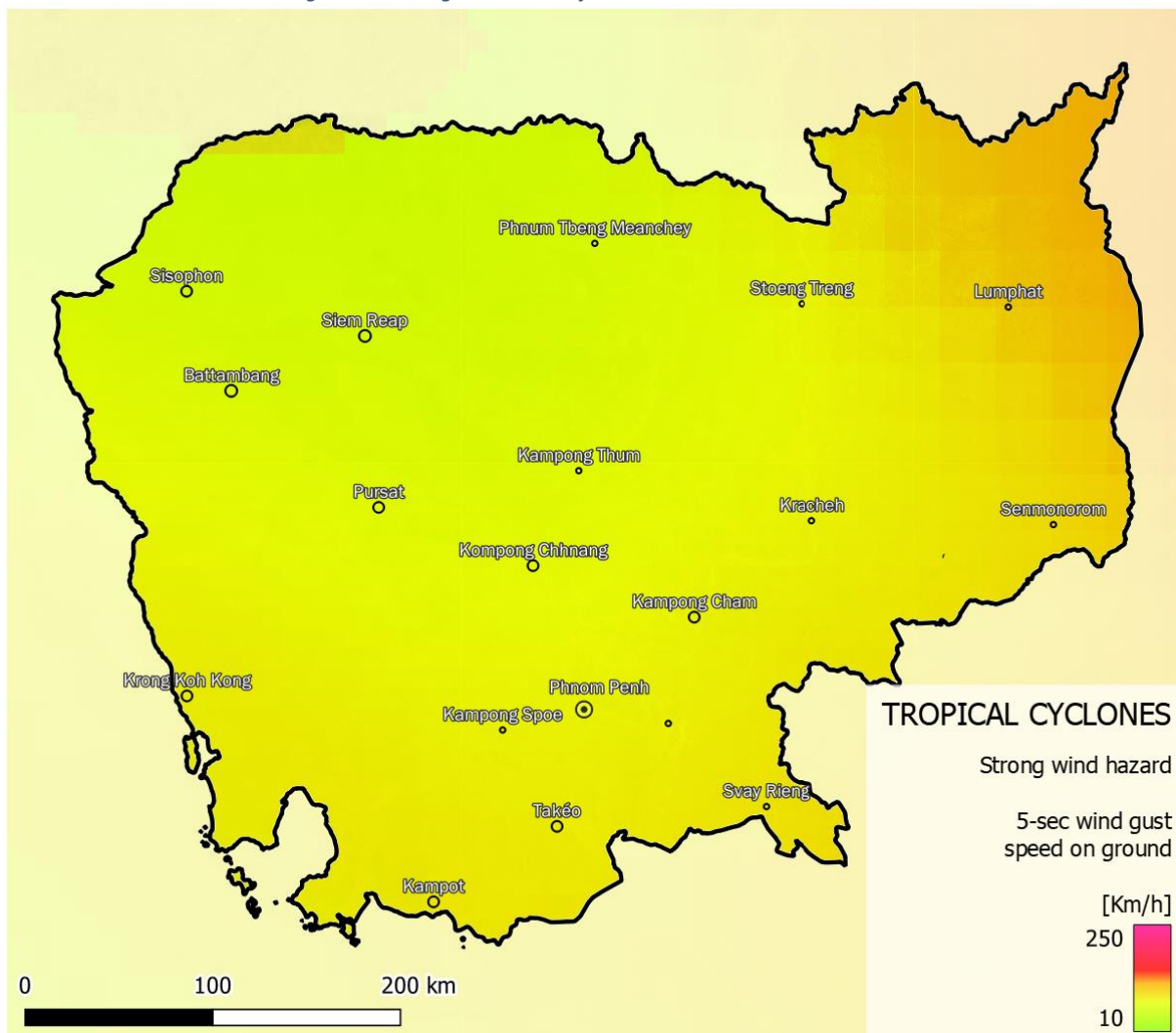


The temperature has increased by 0.18 °C per decade since 1980 (Climate Risk Profile: Cambodia, 2021). Future projections for this area indicate a further temperature rise between 0.5-0.7°C (SSP1/1.9) and 1.0-1.5°C (SSP3-7.0) by 2050 with respect to the baseline (2000-2020), as shown in *Figure 31*.

5.5 Tropical cyclones

Tropical cyclones (Typhoons) in Cambodia occur, on average, about six times a year. The typhoon season in the Pacific usually begins with less severe storms in April and continues until November. The most severe typhoons usually occur in August and September. In 2009, typhoon Ketsana (Cat 2) struck North-eastern Cambodia as one of the most severe storms ever to lash the country, considerably affecting Kampong Thom Province. Over 66,000 families were forced from their homes by flood waters while the death toll reached 43 people. More recently, in September 2022, the passage of Tropical Cyclone Noru (Cat 5) through northern Cambodia caused 16 fatalities due to flooding of the Mekong river. Many houses and a number of roads were damaged, including sections of National Road 9 ([AHA Centre, 2022](#)). About 90 families were evacuated from Mongkul Borei, Banteay Meanchey and Preah Vihear provinces, in the North-West of the country.

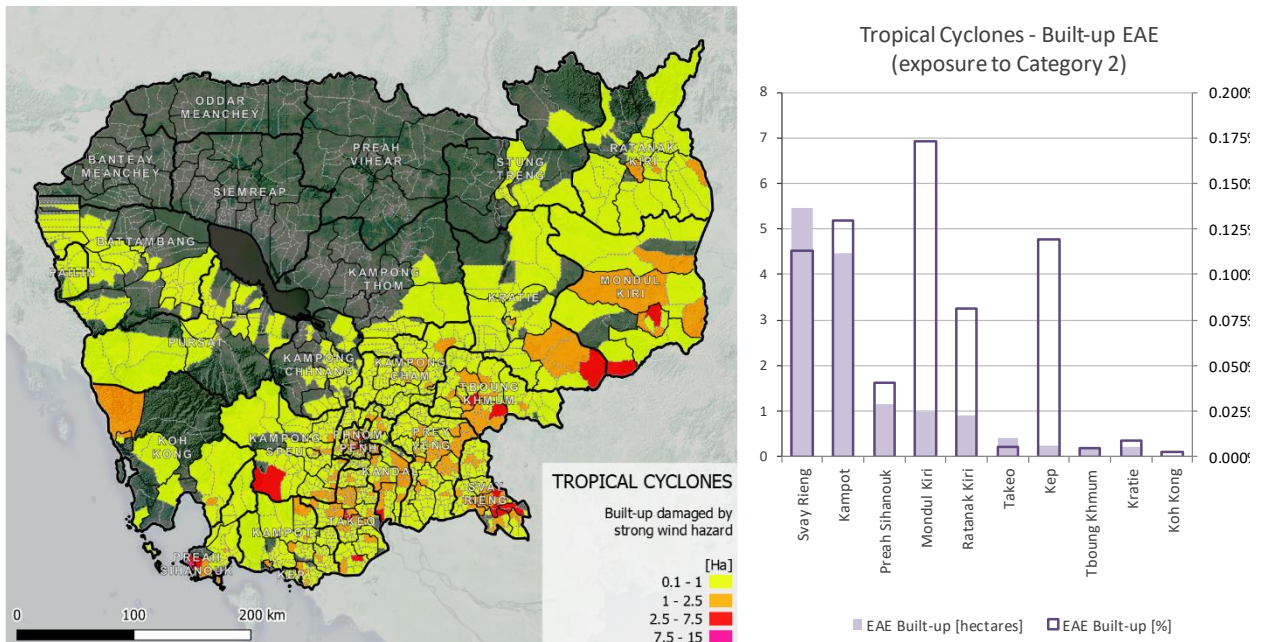
Figure 22: Strong wind hazard from hurricanes across Cambodia



Climate change effects on tropical cyclone hazard is currently poorly understood ([Walsh et al, 2015](#)). With sea level projected to rise between 44 cm (RCP 2.6) to 78 cm (RCP 8.5) by 2100, the impacts of coastal flooding in Cambodia can be significantly higher even if the intensity of tropical cyclones over the country remain relatively constant ([WBG, 2021](#)). The IBTrACS v4 database ([Kenneth et al., 2010](#)), together with STORM 2020 and GAR 2015 wind hazard layers, are used to identify regions that are most exposed to hazardous wind intensity (*Figure 22*). Stronger wind gusts are expected in the Northeastern States (Ratanakiri, Mondolkiri and Kratie), with speeds up to 150 km/h under a return period of 50 years.

According to data, around 2,000 people are expected to be exposed to tropical cyclone hazard in Cambodia every year, particularly in the provinces of Kampot, Svay Rieng and Ratanak Kiri. In terms of built-up areas, an estimate of about 14 ha of built-up area is expected be exposed annual to tropical cyclones, while this number goes up to more than 750 ha of agricultural land (*Figure 23*). Agricultural land is particularly exposed in the provinces of Svay Rieng and Kampot, where about 230 and 223 ha of agricultural land, respectively, are expected to undergo some degree of destruction due to tropical cyclones every year.

Figure 23: Expected Annual Impact over built-up land (ha of land exposed) to strong wind from hurricane events according to tropical cyclone models



5.6 Air pollution

Air pollution is measured by the mean annual surface-level concentrations of PM_{2.5}, which is available from 1998 to 2020 ([van Donkelaar et al, 2021](#)) at 1.1km spatial resolution. This dataset combines data from different sources, including NASA MODIS, MISR, and SeaWiFS observations with the GEOS-Chem chemical transport model into a high-resolution map of air pollution. The dataset combines both human-induced PM_{2.5} emissions, emitted, for instance, by car engines, coal- or natural gas-fired power plants, as well as fireplaces and biomass burning ([NCRD 2014](#)), and natural sources of PM_{2.5}, which include forest fires and desert dust ([McDuffie et al. 2021](#)). These fine particles, smaller than 2.5 micrometers in diameter, pose enormous health risks as they can lodge deeply into the lungs ([WHO 2019](#)). Concentrations of PM_{2.5} over 15 µg/m³ can lead to severe public health consequences (respiratory infections, cardiovascular disease, and lung cancer), especially in densely populated areas. While not a climate hazard in and of itself, air pollution can be affected by climate change ([UCAR 2022](#)), but can also affect local climate: drier conditions can promote dust transport from soil; wildfires can increase the local dust concentration; high dust can alter the heat intake from the sun and thus affect temperatures. *Figure 24* depicts the average 1998-2019 concentration of fine particulate matter (PM 2.5) in Cambodia.

Linking pollution hazard to population exposure and using the mortality impact function associated with high PM_{2.5} concentrations (*Figure 25*) helps to better identify places with the largest absolute number of people exposed to health issues and reduced life expectancy. The exposure is found to be higher in highly urbanized areas of Phnom Penh, Battambang, Kandal and Siemreap, where thousands of citizens are at increased mortality risk due to air pollution every year. Overall, approximately 2 million Cambodians to be exposed to some degree of risks due to air quality.

Figure 24: Air pollution hazard (mean PM 2.5) across Cambodia

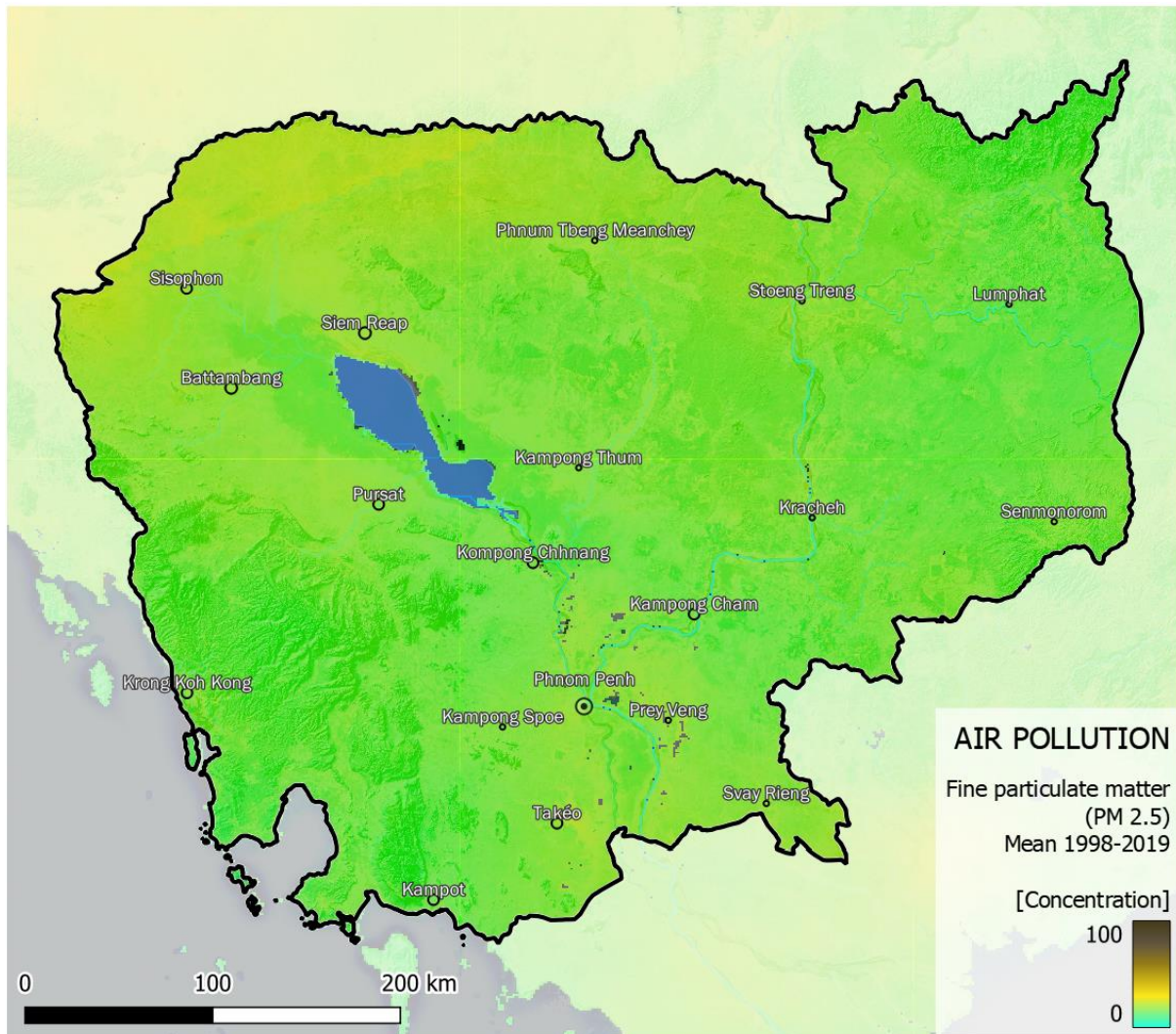
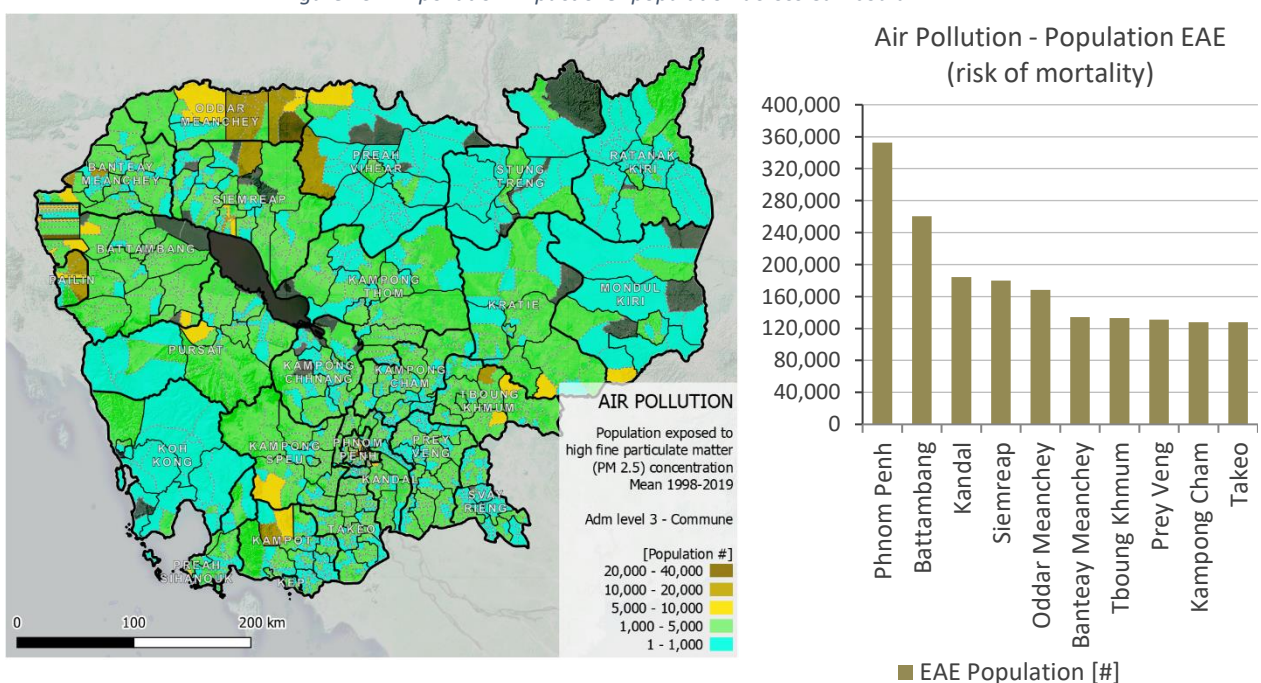


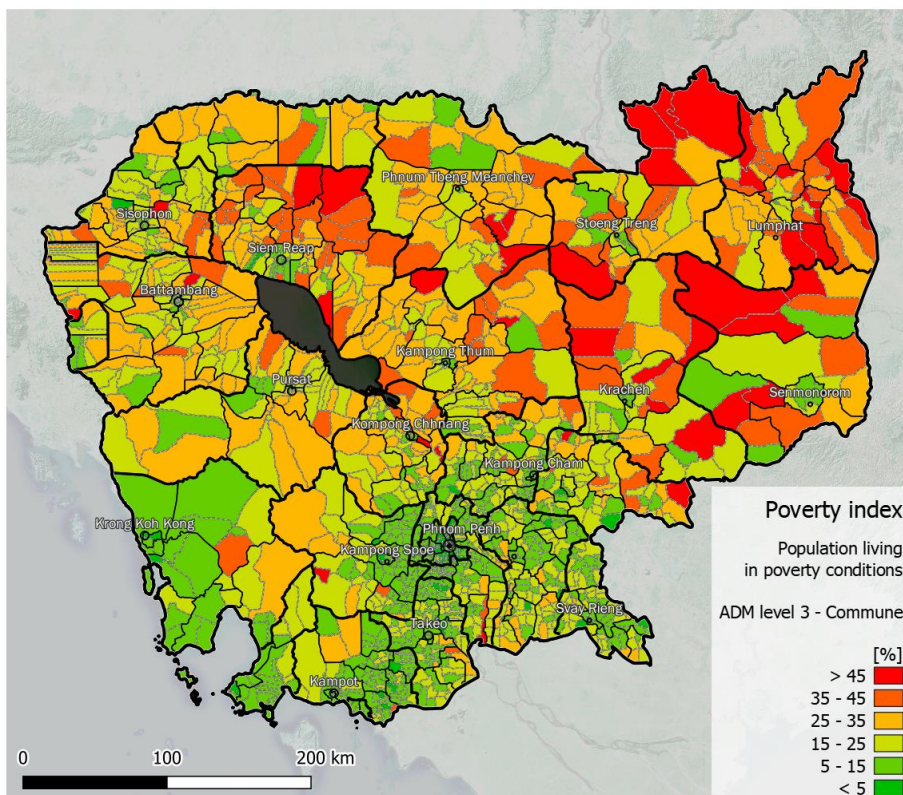
Figure 25: Air pollution impact over population across Cambodia



6 Risk and Poverty – Bivariate maps

The distributional impact of climate risks can be examined by overlaying poverty maps (National Institute of Statistics, 2022) shown in Figure 26, on built-up asset and agricultural land EAE and EAI maps produced in the earlier section. These results are visualized using a series of bivariate maps that show the locations where risk is most likely to translate into severe impacts on the poorest and vulnerable households.

Figure 26: share of population living in poverty conditions in 2020 based on poverty maps for ADM3 level (Communes).



Poverty maps, produced using the 2019 household consumption survey data and small area estimation methods, provide relative and absolute number of poor individuals per commune. Poverty maps are combined with EAE/EAI maps to then generate bivariate maps. These maps provide ranks explained by a 3x3 matrix, resulting in 9 possible scores ranging from low-risk / low-poverty to high-risk / high poverty. The matrix is built by classifying poverty indicators into three quantiles and dividing risk indicators (EAE/EAI) of each hazard type into groups shown in *Table 5*. Classification of total exposure on an administrative unit is done both on the basis of absolute numbers as well as ratios. In order to better capture the spatial variation in the expected disaster risk. For instance, as severe fluvial flooding and landslides represent very localized threats, the classification is based on total counts. In comparison, heat waves, droughts and air pollution are more widespread across geographic units and therefore classified into groups based on proportions.

Table 5: Selected risk classification approach by hazard

Risk indicator	Unit	Metric	Risk Classification		
			Low	Medium	High
Flood x Population	EAI [#]	Total count	0.01 - 100	100 – 1,000	> 1,000
Flood x Built-up	EAI [Ha]	Total count	0.01 – 1	1 – 10	> 10
Flood x Agri land	EAE [Ha]	Total count	0.01 - 100	100 – 1,000	> 1,000
Landslide x Population	EAE [#]	Total count	0.01 - 100	100 – 2,000	> 2,000
Landslide x Built-up	EAE [Ha]	Total count	0.01 - 1	1 – 20	> 20
Tropical Cyclone x Population	EAI [#]	Total count	0.01 – 10	10 – 50	> 50
Tropical Cyclone x Built-up	EAI [Ha]	Total count	0.01 – 0.1	0.1 – 0.3	> 0.3
Tropical Cyclone x Agri land	EAE [Ha]	Total count	0.01 - 10	10 – 100	> 100
Drought x Agri land	EAI [%]	Ratio	1 - 5	5 - 15	> 15
Heat stress x Population	EAE [#]	Ratio	1 – 10,000	10,000 – 30,000	> 30,000
Air pollution x Population	EAE [#]	Ratio	1 – 5,000	5,000 – 15,000	> 15,000

The expected annual impact of river and coastal floods on population mortality (*Figure 27, left*), damage to built-up assets (*Figure 27, right*), and annually exposed cropland and pasture (*Figure 28*) is overlaid with poverty maps. The wealthy regions around the capital are expected to have better means to cope with flood disaster risk, while the poorer areas along the Mekong valley are expected to be at higher risk. The risk of climate change on the poorest populations are most concentrated in the north-western parts of Cambodia. Poorer households with higher risk of flooding likely reside in hazard-prone areas, with poorer insurance and adaptive or preventive measures against high water.

Figure 27: Bivariate map between poverty (number of poors, WB data) and EAI from river flood hazard over population (left) and built-up (right)

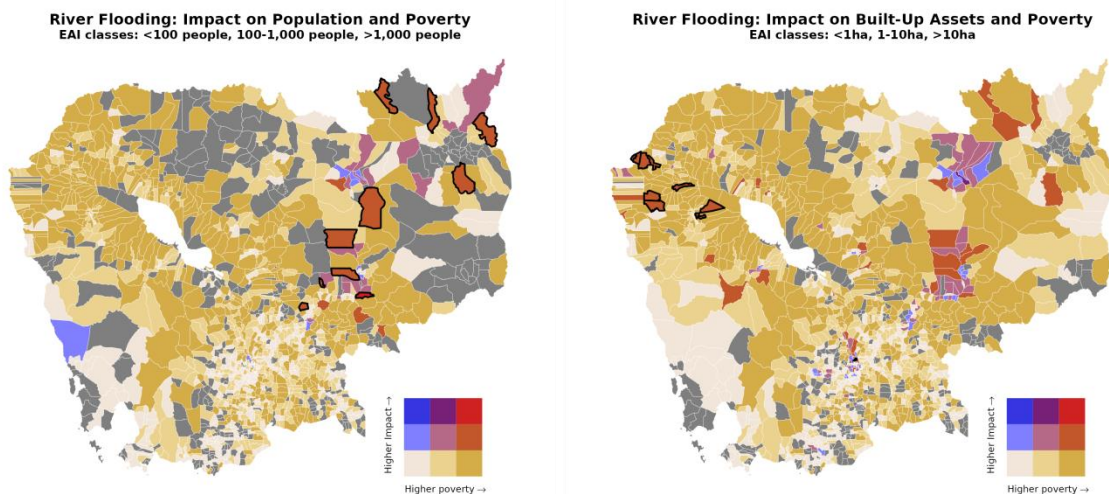


Figure 28: Expected annual exposure of agricultural land to river and coastal floods and poverty (number of poors, WB data)

The effects of flooding on agricultural land and poorest households is highest in the north-western parts of the country. Rural poorer, especially subsistent farmers, located in these regions are most at risk of livelihood related shocks in these regions. In the central floodplain areas, river flooding can be further compounded by other hazards, such as tropical cyclones, droughts, and heat stress. Adaptive measures therefore required to protect these at-risk residents.

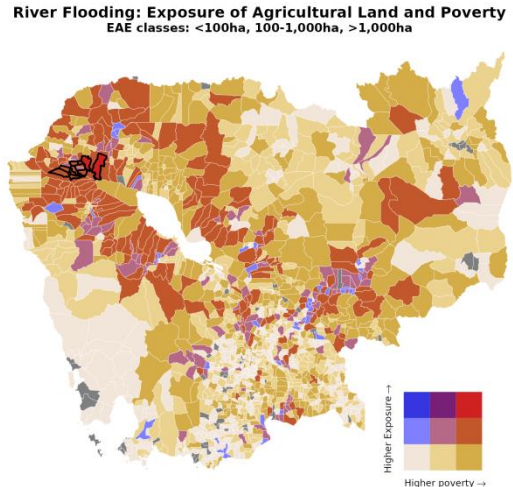


Figure 29: Expected annual exposure of agricultural land to drought and poverty (number of poors, WB data)

Recurring drought events affect large areas of the Cambodian territory, but are particularly frequent in the central area around the valleys of the Mekong and the Tonle Sap rivers (Figure 29). Historically, these are the same areas that are also impacted by fluvial floods and heat stress, thus the compounding effect of frequent agricultural drought (more than once every about five years) and high poverty poses distributional risk from climate change.

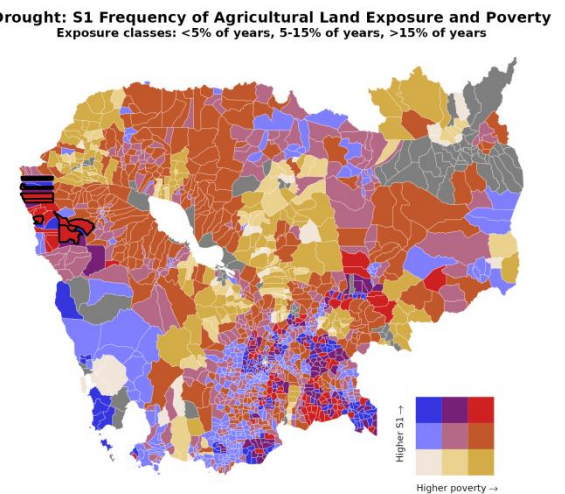
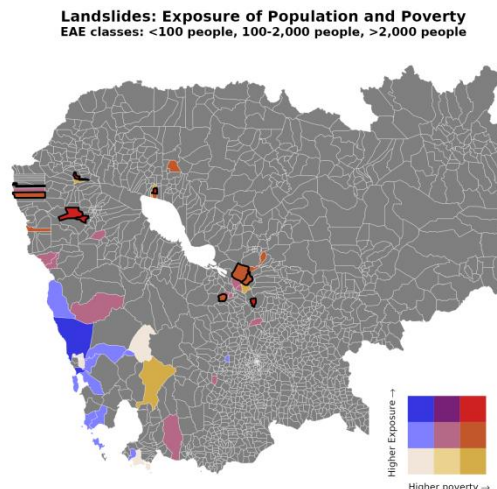


Figure 30: Expected annual exposure of population to landslide hazard and poverty (number of poors, WB data)

In general, most of the country is not particularly exposed to landslide hazard. However, some specific areas are exposed potentially significant landslide hazard, mostly around the mountainous southwestern areas of Cambodia. However, a few municipalities exposed to landslides are also likely to be poorer (Figure 30).



With the exception of municipalities and areas located on northeast and southwest of Cambodia, heat stress is felt throughout all the country and affects nearly all Cambodians with relative high frequency and intensity.

In the relatively less wealthy northern and western Cambodian provinces, high rates of poverty coincide with a large population exposure to heatwaves annually – with over 50,000 inhabitants expected to face extreme heat stress each year while in the lowest third of relative wealth (*Figure 31*).

The communities in these areas are most at-risk of the negative health consequences of extreme heat stress. Around wealthier urban centres of Phnom Penh and Siem Reap, richer households are exposed to heat stress. However poorest households living in such urban centers are therefore particularly at-risk of the negative consequences of heat to their health and livelihoods as opportunities to cope with heat hazards is likely considerably lower than richer households in the same area.

Figure 31: Expected annual exposure of population to heat stress and poverty (number of poors, WB data)

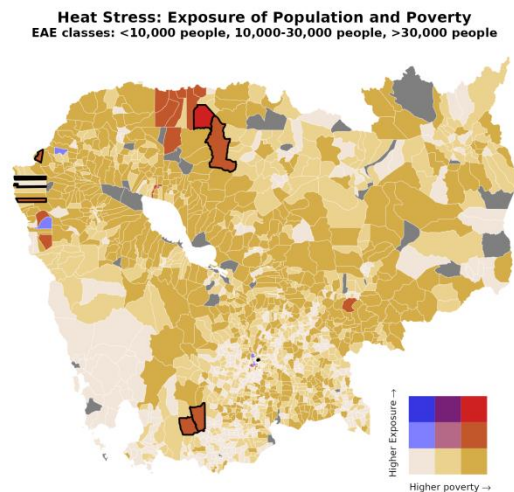
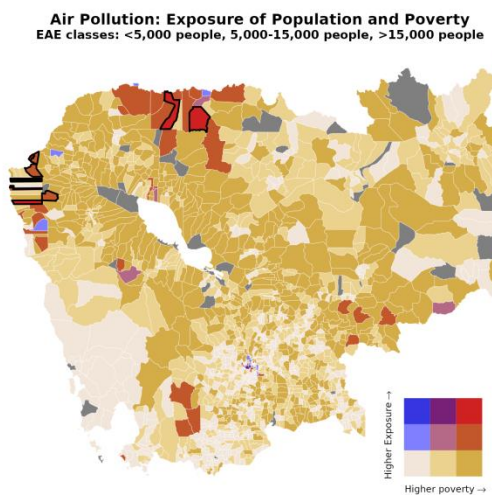


Figure 32: Expected annual impact on population of air pollution and poverty (number of poors, WB data)



Poorer households in the north-western provinces of Cambodia have the highest risk from high PM2.5 concentrations (*Figure 32*). This is particularly the case of municipalities in the provinces of Oddar Meanchey and Battambang, where over 50,000 residents in the lower third of relative wealth are annually at risk of some level of sanitary consequences due to air quality.

Tropical cyclone hazard hits Cambodia mainly on its eastern and southern borders (*Figure 33*). The provinces that are traditionally more exposed to this type of hazard are Ratanak Kiri, Mondul Kiri, Preah Sihanouk, Svay Rieng, and Kampot,. Densely populated areas and relatively wealthier urban centres, including Phnom Penh and Siem Reap, are not expected to face significant consequences from tropical cyclone according to the historical analysis.

Figure 33: Expected annual exposure of population to tropical cyclones and poverty (number of poors, WB data)

Tropical Cyclone: Exposure of Population and Poverty
EAE classes: <10 people, 10-50 people, >50 people

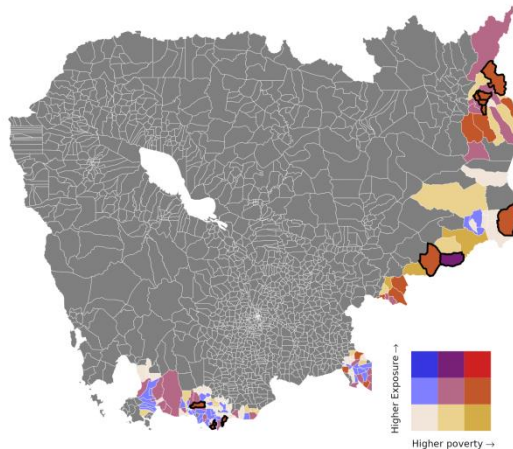
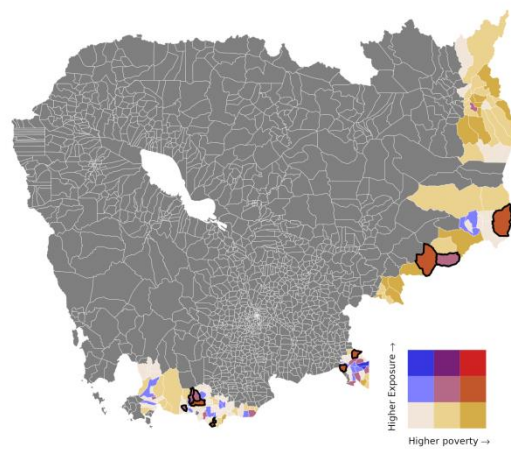


Figure 34: Expected annual exposure on built-up area to tropical cyclones and poverty (number of poors, WB data)

Tropical Cyclone: Exposure of Built-Up Assets and Poverty
EAE classes: <0.1ha, 0.1-0.3ha, >0.3ha



A similar pattern emerges for built-up areas at risk when overlaid to mean wealth values (*Figure 34*). Once again, the provinces of Svay Rieng, Kampot, Preah Sihanouk, Mondul Kiri, and Ratanak Kiri are particularly exposed to tropical cyclones, with at least 1 ha of built-up area is expected to be exposed to damages caused by tropical cyclones.

7 Hazard projections: climate indices

The climate indices associated with presented natural hazards are discussed below. Each of these mapping ensembles has a similar structure. The gridded historical mean over the baseline period 1995–2014 is shown in the top left, with the historical average over this period shown on the map at the bottom left. The second, third and fourth columns then represent the projected anomalies for the climate variables under SSP1 – 2.6 (second column), SSP2 – 4.5 (third column), and SSP5 – 8.5 (fourth column). The top row shows the gridded standardised anomalies derived from CMIP6 for our time horizon 2041–2060, while the bottom row shows the average standardised anomaly for each province in Cambodia. Below the maps, for each climate variable, the historical variation during the baseline period is shown, together with the projected future anomalies for the three SSPs.

7.1 Rainfall indices

Four climate indices are assessed to estimate the change in extreme rainfall trends, which could ultimately affect flood and landslide hazards: annual number of consecutive wet days (CWD, *Figure 35*), annual days of rainfall with over 10mm of precipitation (R10mm, *Figure 36*), maximum precipitation over five days (Rx5day, *Figure 37*), precipitation amounts during extremely wet days (R99p, *Figure 38*), and the projected sea level rise (SLR, *Figure 39*).

The historical baseline shows increasing wet conditions in Cambodia along the coastline and also to the North-eastern part of the country, consistent across the four precipitation-related variables. Both for short-term, extreme rainfall events, as well as longer-term precipitation periods, the central floodplains of Cambodia show the lowest precipitation volumes. In contrast, the South-western part of the country, and especially the area along the coastline of Cambodia, shows the overall highest annual number of consecutive wet days, days with rainfall over 10mm, extreme precipitation events, and volumes of rainfall over a five-day period.

Looking at the climate projections for these four precipitation indices, a more complex yet consistent spatial pattern emerges. For days with rainfall over 10mm, maximum 5-day precipitation, and extreme wet day precipitation, a strong positive signal in standardised anomalies for the 2041–2060 period compared to the 1995–2014 baseline is observed over the central plains of Cambodia, particularly over the Siem Reap basin, indicating that precipitation events may be increasing in intensity over these areas. Interestingly, however, is the fact that consecutive wet days shows a negative standardised anomaly signal, indicating that the potential increase in rainfall intensity over the central areas of Cambodia is not due to prolonged rainfall period, but likely rather due to more intense extreme rainfall events, being a worrisome result for flood risk in the country. Adaptive measures to prevent an increase in mortality and damage to built-up and agricultural assets thus will need to be taken. These trends are considerably starker for higher-emission future scenarios, in particular SSP5 – 8.5.

Figure 35: Climate indices - Consecutive Wet Days (days/year) for Cambodia

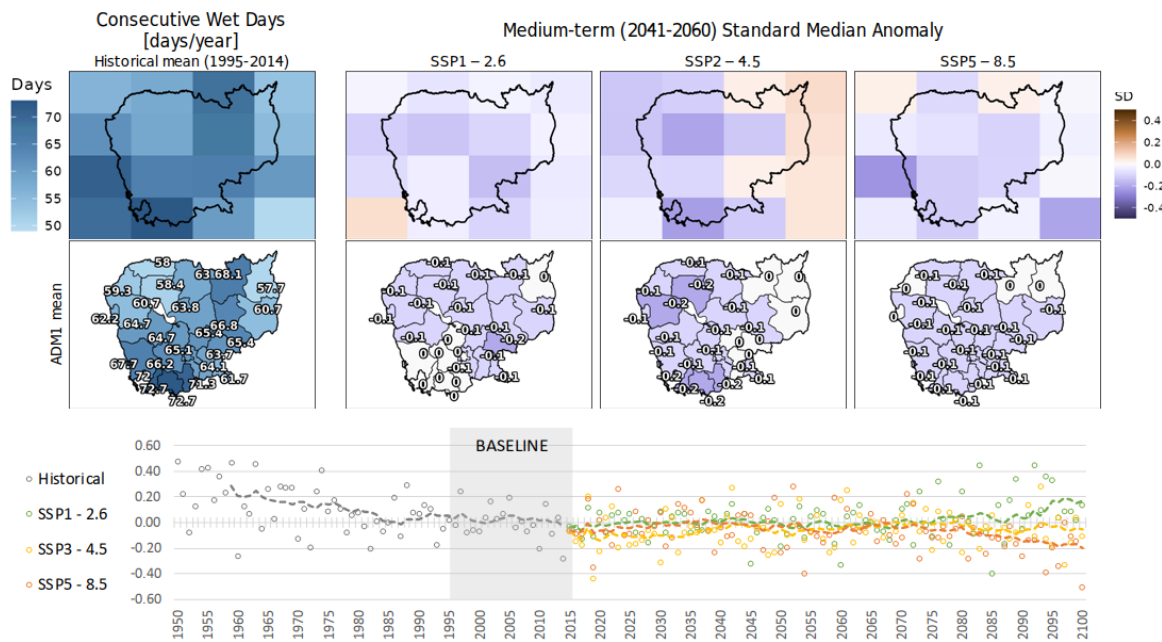


Figure 36: Climate indices - Rainfall over 10mm (days/year) for Cambodia

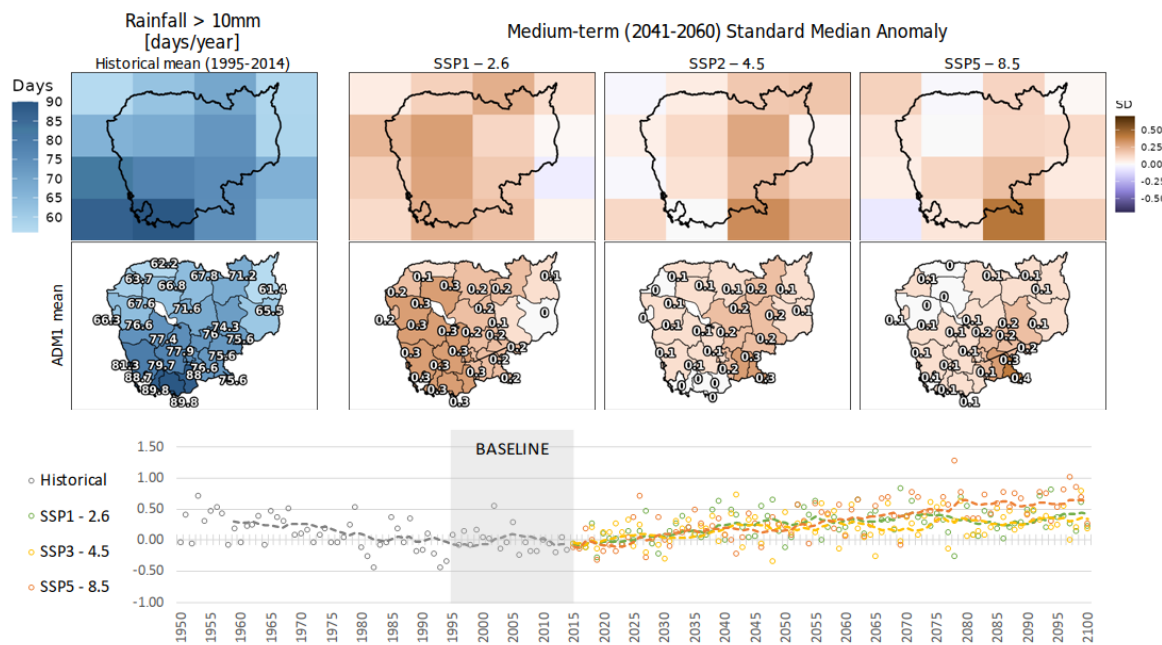


Figure 37: Climate indices - Maximum 5-day Precipitation (mm/year) for Cambodia

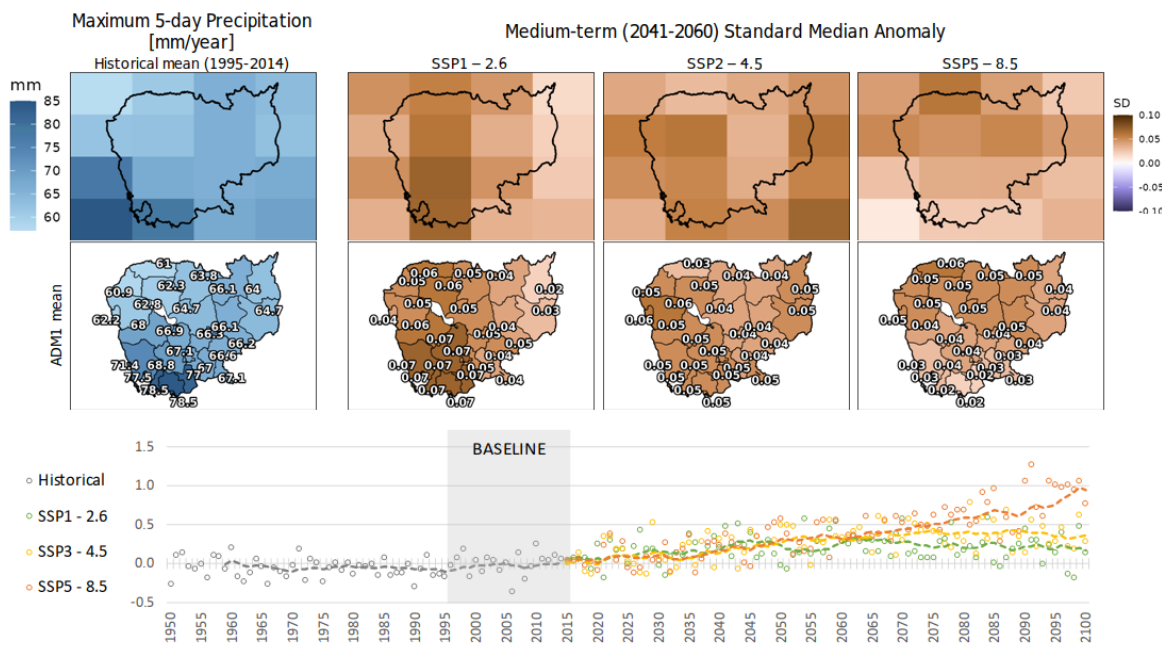
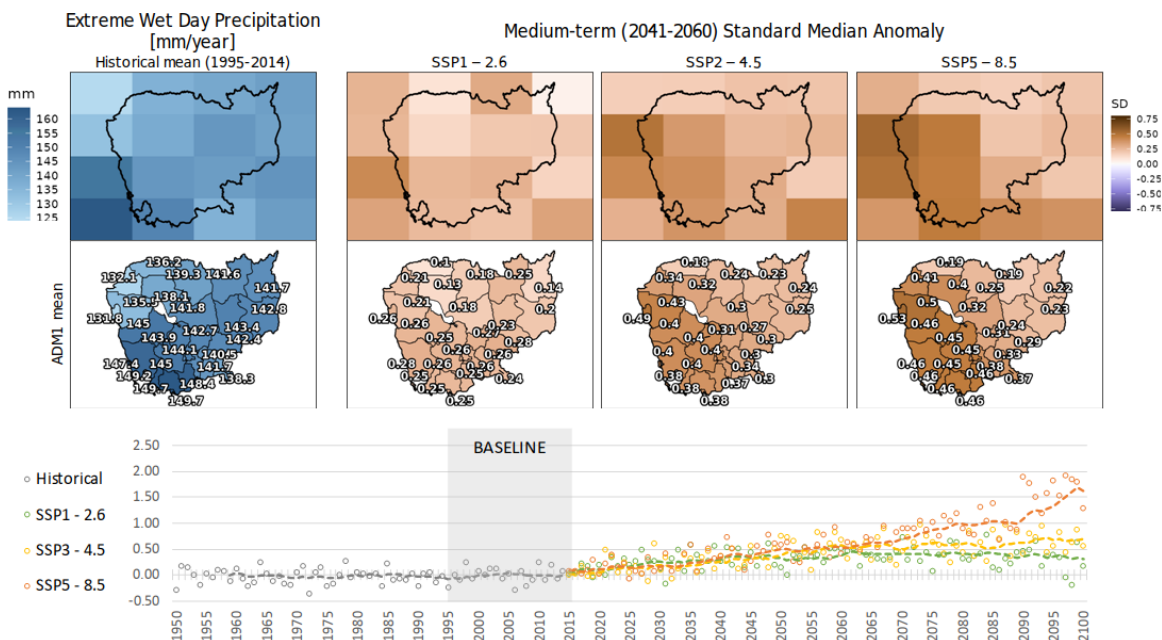
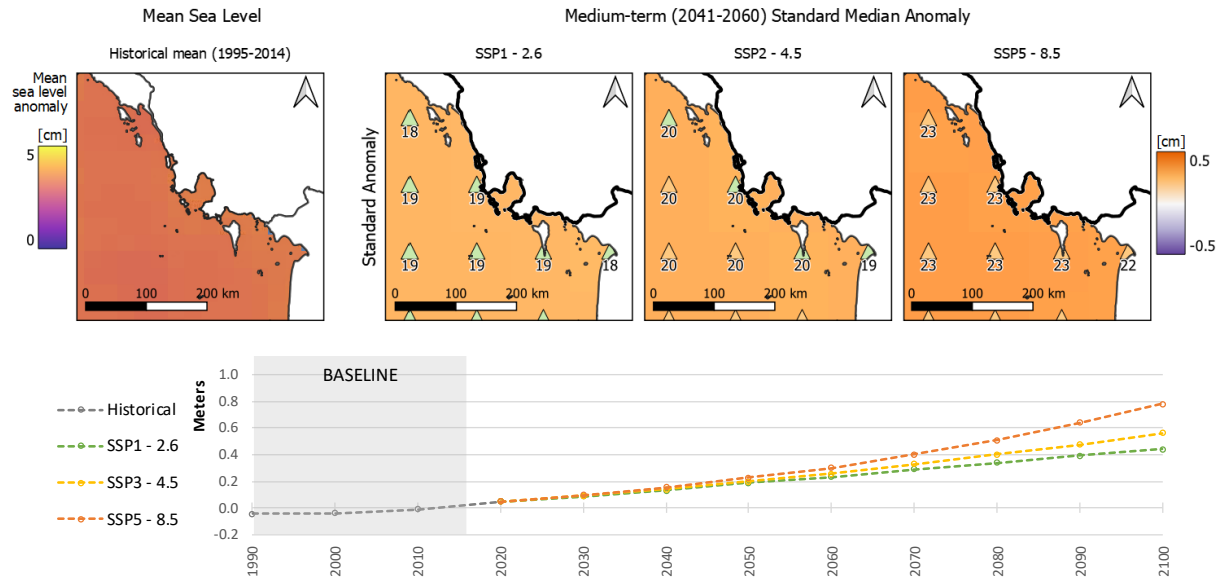


Figure 38: Climate indices - Extreme Wet Day Precipitation (mm/year) for Cambodia



Along the coastlines of Cambodia, sea level rise raise is a point of serious concerns, particularly for the provinces of Koh Kong and Preah Sihanouk, facing the strongest rise in sea level rise by mid-century, of at least 19 cm under all climate change scenarios. By the end of the century, however, sea level could rise by 40 cm to 80 cm for the scenarios SSP1-2.6 and SSP5-8.5, respectively.

Figure 39: Climate indices - Average Sea Level Rise (cm)



7.2 Drought indices

Two variables underpin the projection of changes in drought patterns: the *number of consecutive dry days per year* (CDD, *Figure 40*), and the *12-month Standardized Precipitation-Evapotranspiration Index* (SPEI, *Figure 41*). The SPEI has been found to be closely related to drought impacts on ecosystems, crop, and water resources, and has been designed to take into account both precipitation and potential evapotranspiration in determining drought ([World Bank 2022](#)). It is important to note that negative SPEI values indicate drier than normal conditions, while positive values indicate wetter than normal conditions. The mapping ensembles for these drought-related variables follow a similar design to the precipitation-related variables, again with the 1995-2014 period as a historical baseline.

The historical baseline shows that the North-western region of Cambodia has the largest number of CDD (around 70 days/year), while the central floodplains around the Mekong and the Siem Reap valleys account for about 50 days of CDD every year, in average. The climate projections of CDD and offer a complementary, yet slightly different, spatial picture of the forecasted trends. The SPEI shows little change in standardised anomaly under any of the SSPs compared to the baseline for most of Cambodia, with exception of the southeast part of the country and under the stronger climate change scenario – SSP8.5. There, an increase in wetness is expected through positive standardised anomalies. For the rest of the country, this suggests that little change is expected in agricultural drought patterns during the period 2041-2060 compared to the 1995-2014 reference period, yet inter-annual variability cannot be ruled out, particularly during strong El Nino years. Indeed, more dispersed in time yet more intense rainfall seems to be more likely in Cambodia under future climate conditions, as highlighted by the increased positive standardised anomaly of CDD under the future climate scenarios and the precipitation projection results discussed above.

Figure 40: Climate indices – Consecutive Dry Days for Cambodia

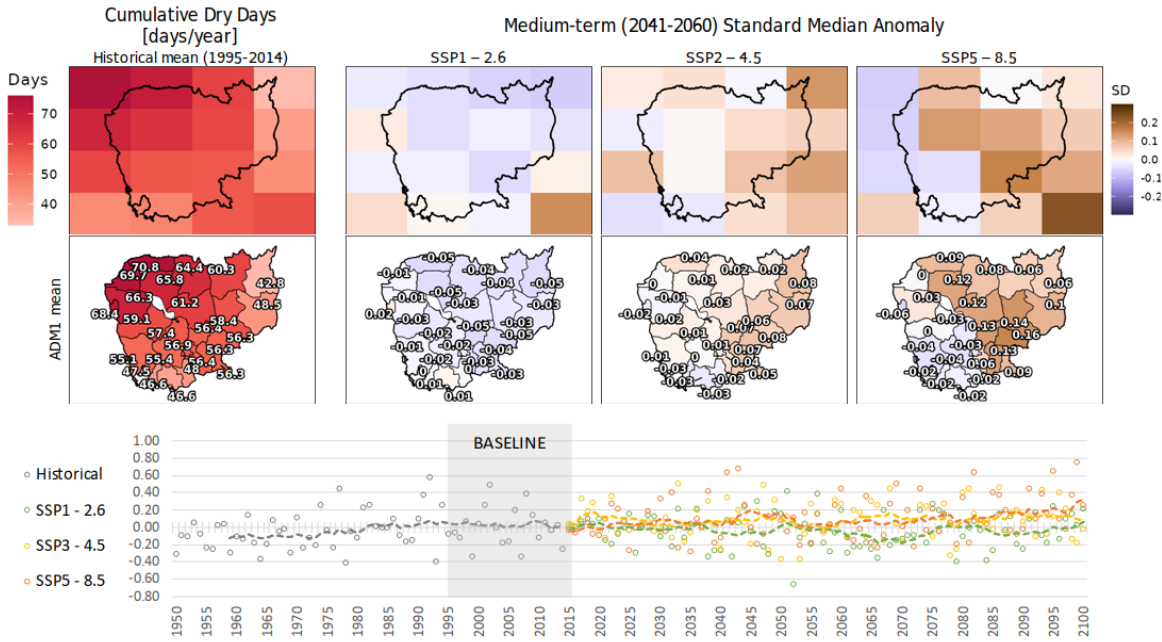
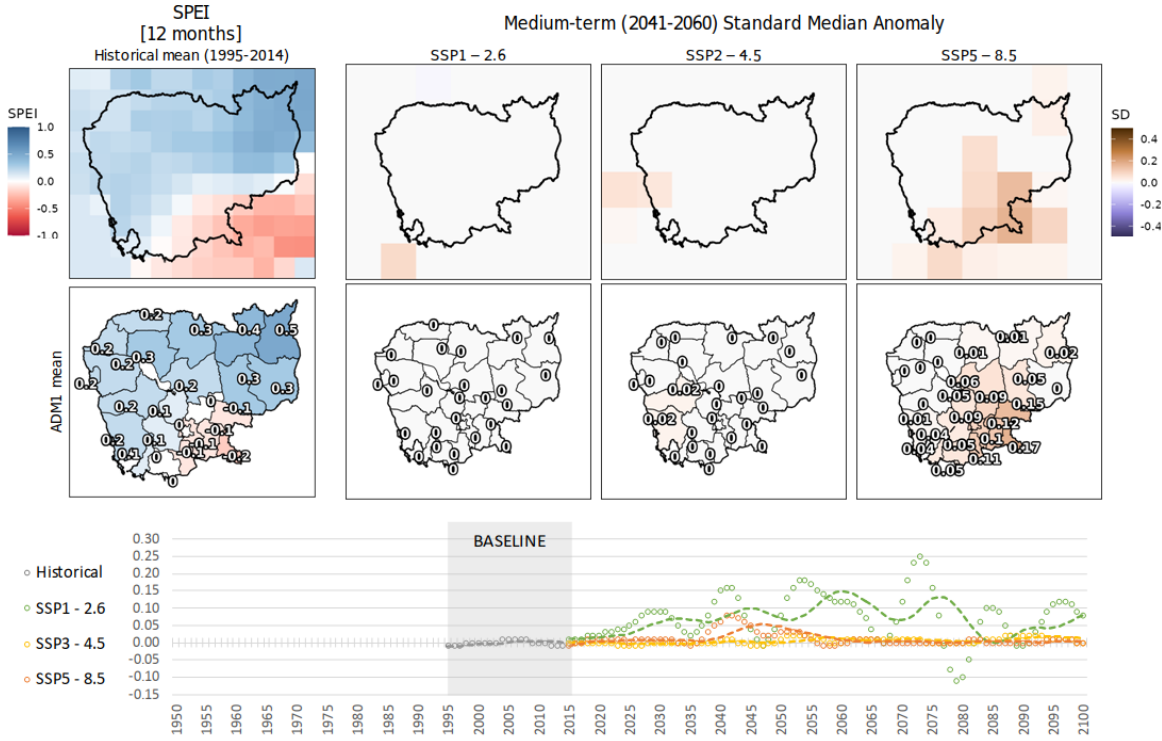


Figure 41: Climate indices – Standard Precipitation-Evapotranspiration Index for Cambodia



7.3 Heat indices

The change in heat patterns under the three climate change scenarios is estimated by looking at the projections of the *WBGT heat index*. Changes in the frequency (i.e., number of days) of extreme heat events are analyzed. Of notable interest is the increased frequency in the occurrences of both the moderate (WBGT >23°C, Figure 42) and the extreme (WBGT >30°C, Figure 43) heat stress events in the region, which can potentially translate into unprecedented heat stress and mortality (even under the lower emission scenario). The long-term trend of the heat indices is particularly worrisome. Under

SSP1, only a slight to moderate increase is expected in the total number of days over WBGT 23°C and 30°C with the chance to reduce the anomaly again by the end of the century; while both SSP2-4.5 and SSP5-8.5 project a steady and significant increase of hot days and especially extremely hot days, worsening the already high heat stress risk.

The most vulnerable people to heat-related illnesses are workers who spend a substantial portion of the shift outdoors and those who work in hot and humid environment indoors: agricultural workers, miners, fishermen, construction/building workers, electricians, landscapers, ground maintenance, and factory workers ([Bourbonnais et al., 2013](#); [Lucas et al., 2014](#)). Considering that the agriculture sector employs the large majority of the active labor force and accounts for a large share of the gross domestic product, the projected heat stress threatening the workers' health can reduce productivity and undermine the region's economic development.

Under all three SSPs, the standardized anomalies of heat are forecasted to significantly increase relatively to the 1990-2010 reference base. This increase is considerably stronger under higher-emission future scenarios. Looking at extremely hot days with a WBGT of over 30 degrees Celsius, the historically warmer center of the country is set to see a strong increase in extreme heat events – with the historically colder southwest also seeing a considerable increase, particularly along the coastline. The projected rise in temperatures is concerning, as it indicates increased heat stress across Cambodia by the 2041-2060 period, potentially putting even more lives at risk and raising awareness for the most vulnerable, such as children and the elderly. The fact that this increase is fairly homogenous across the entirety of the country's territory raises particular questions on adaptation and prevention for the urban environments, where heat stress can be amplified by the "[heat island](#)" effect.

Figure 42: Climate indices – Days Wet-Bulb Globe Temperatures (WBGT °C) over 23°C

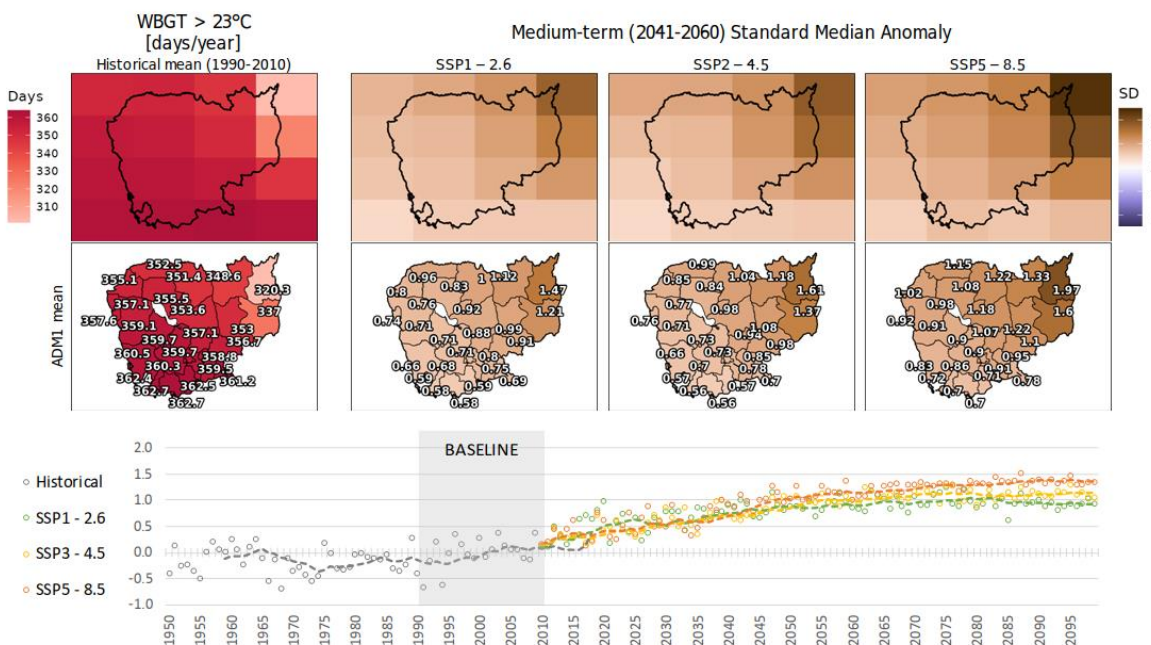
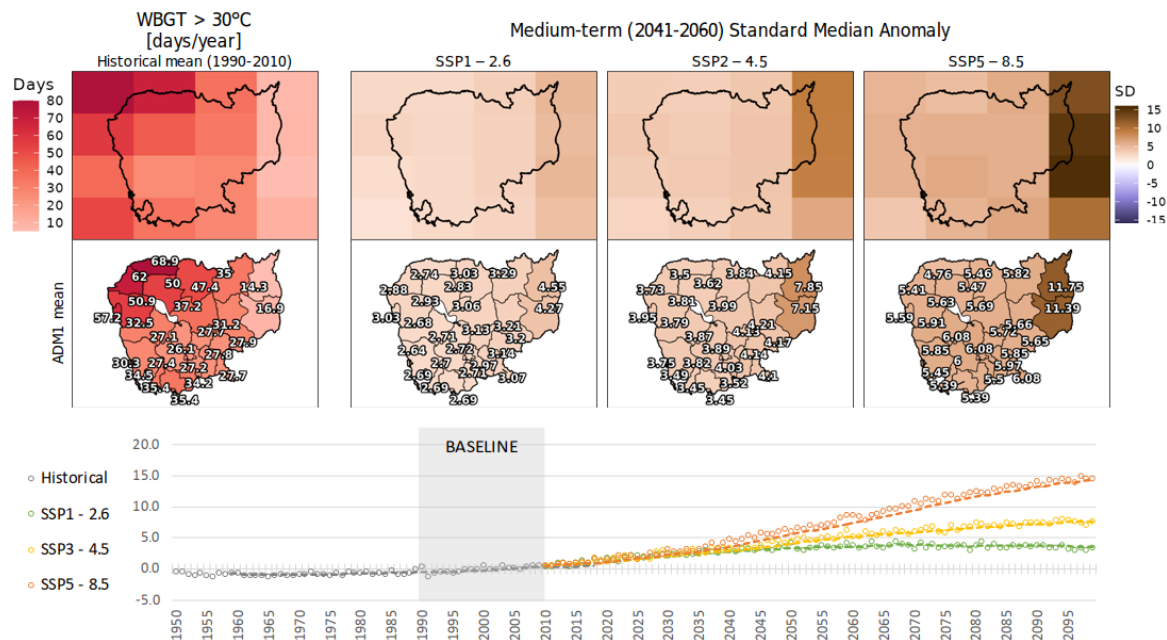


Figure 43: Climate indices – Days Wet-Bulb Globe Temperature (WBGT °C) over 30°C



8 Annex 1 – Hazard models

1.1 Fluvial floods

Name	Fathom flood hazard maps v2
Developer	Fathom
Hazard process	Fluvial flood
Resolution	90 m
Analysis type	Probabilistic
Frequency type	Return Period (10 RPs)
Time reference	Baseline (1989-2018)
Intensity metric	Water depth [m]
License	Commercial (acquired by World Bank)
Notes	“Undefended scenario” option is selected for the analysis.

1.2 Coastal floods / Storm surges

Name	Aqueduct flood hazard maps
Developer	WRI - Deltares
Hazard process	Coastal flood
Resolution	1 km
Analysis type	Probabilistic
Frequency type	Return Period (10 RPs)
Time reference	Baseline (1960-1999)
Intensity metric	Water depth [m]
License	Open data
Notes	Includes effect of local subsidence.

1.3 Agricultural droughts

Name	Agricultural Stress Index (ASI)
Developer	FAO
Hazard process	Agricultural drought
Resolution	1 km
Analysis type	Deterministic (remote sensing)
Frequency type	Occurrence frequency
Time reference	Baseline (1984-2020)
Intensity metric	Percentage of crop and pasture land affected by drought conditions across baseline period.
License	Open data
Notes	Aggregated from annual data scale.

1.4 Heat stress

Name	Global extreme temperatures (WBGT)
Developer	VITO
Hazard process	Extreme heat
Resolution	10 km
Analysis type	Probabilistic
Frequency type	Return Period (3 RPs)
Time reference	Baseline (1981-2010)
Intensity metric	Wet Bulb Globe Temperature [°C]
License	Open data
Notes	Simplified wet bulb globe temperature defined as: $WBGT = 0.567 T + 0.393 VP + 3.94$ with T the air temperature (in °C) and VP the vapour pressure (in hPa) (WMO, 2015)

1.5 Tropical Cyclones

Name	STORM tropical cyclone wind speed
Developer	STORM – Deltares
Resolution	10 km x 10 km
Analysis type	Probabilistic
Frequency type	Return Period (6 RPs)
Time reference	1980-2018
Intensity metric	Maximum wind speeds [m/s]
License	Open data
Notes	Data is available for every ocean basin. Return periods were empirically calculated using a Weibull's distribution.

Name	IBTrACS v4
Developer	NOAA - NCEI
Resolution	Individual events
Analysis type	Observations
Frequency type	none
Time reference	1980-2022
Intensity metric	Category, wind speed
License	Open data

1.6 Air pollution

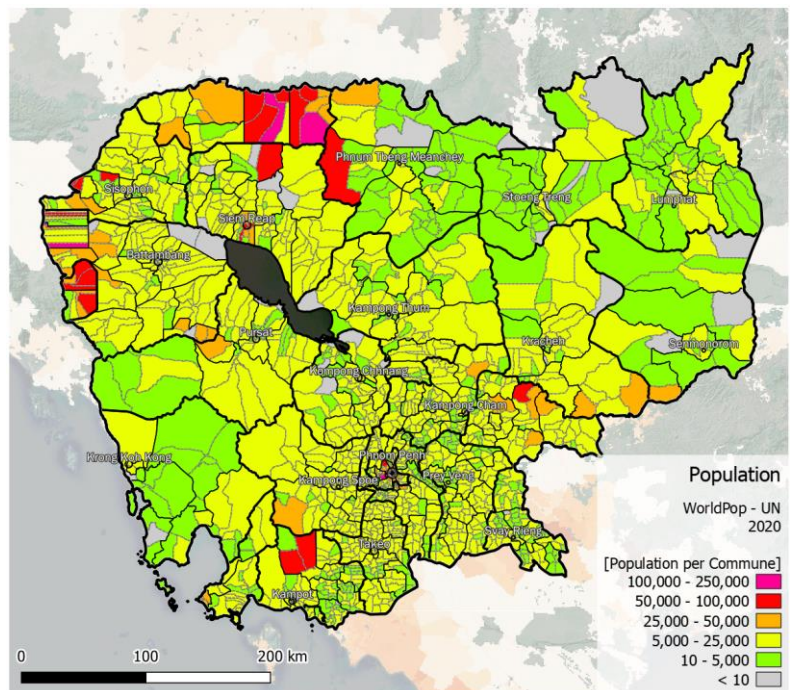
Name	ACAG surface PM2.5
Developer	Van Donkelaar et al., Washington University
Resolution	1 km x 1 km
Analysis type	Deterministic
Time reference	1998-2020
Intensity metric	PM 2.5 concentration
License	Open data
Notes	Based on MODIS, MISR, SeaWiFS data. Aggregated from annual data scale.

9 Annex 2 – Exposure models

1.7 Population

Name	WorldPop
Developer	Southampton university
Format	Raster grid
Resolution	100 m
Time reference	2020
Metric	Population count
License	Open
Notes	Constrained to built-up (2020)

Figure 44: WorldPop 2020 population model for Cambodia – by ADM3 level



1.8 Built-up

Name	World Settlement Footprints
Developer	ESA
Format	Raster grid
Resolution	10 m
Time reference	2019
Metric	Presence of built-up (binary)
License	Open

1.9 Land cover and land use

Name	ESA WorldCover
Developer	VITO and consortium for ESA
Format	Raster
Resolution	10 m
Time reference	2020
Metric	Land cover classes
License	Open

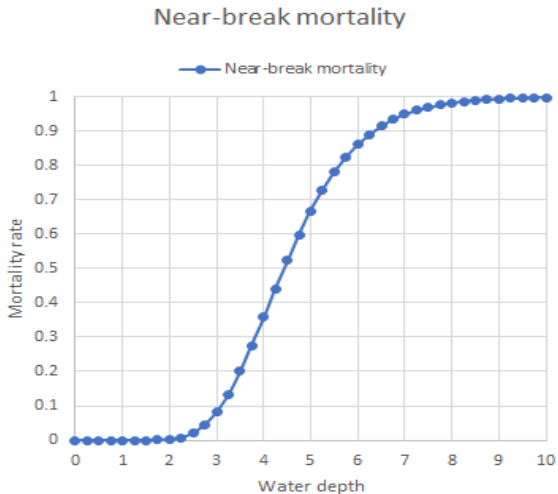
10 Annex 3 - Vulnerability functions, thresholds, and calculations

10.1 Floods (river and coastal)

Population: Generalized mortality function for people located close to dam break ([Jonkman et al. 2008](#))

Approximated by:

$$y = \frac{0.985}{1 + e^{(6.32 - 1.412x)}}$$

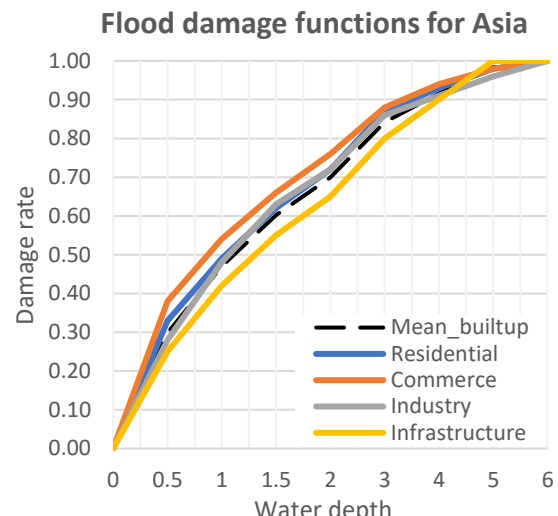


Built-up: regionalized (continent) impact function for land cover categories ([Huizinga et al. 2017](#))

- Mean function for built-up area classes, including residential and industrial categories

Approximated by:

$$y = 0.506x - 0.1(x^2) + 0.00723(x^3)$$



Agriculture: classification of exposure for water depth > 0.5 m

Class	Water depth range (m)
C1	0.01 - 0.15
C2	0.15 - 0.5
C3	0.5 - 1
C4	1 - 1.5
C5	1.5 - 2
C6	> 2

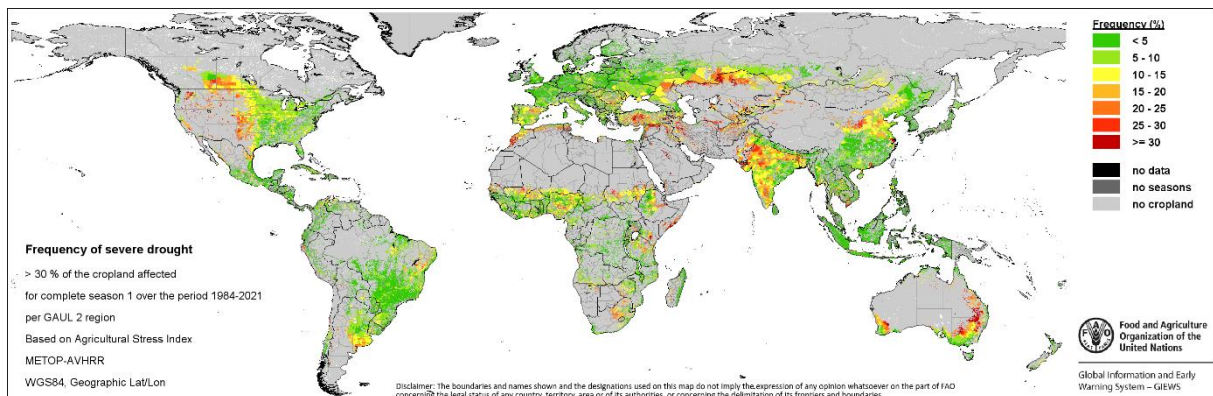
10.2 Landslides

Built-up and Population: ARUP index classification. “High hazard” class (C3) is plotted in maps; if empty, C2 (“medium hazard”) is plotted.

ARUP intensity index	Class
< 0.001	Low
0.001 – 0.01	Medium
> 0.01	High

10.3 Drought (water stress on agriculture)

Agriculture: [FAO ASIS](#) standard classification; frequency of impact over >30% or >50% of cropland.



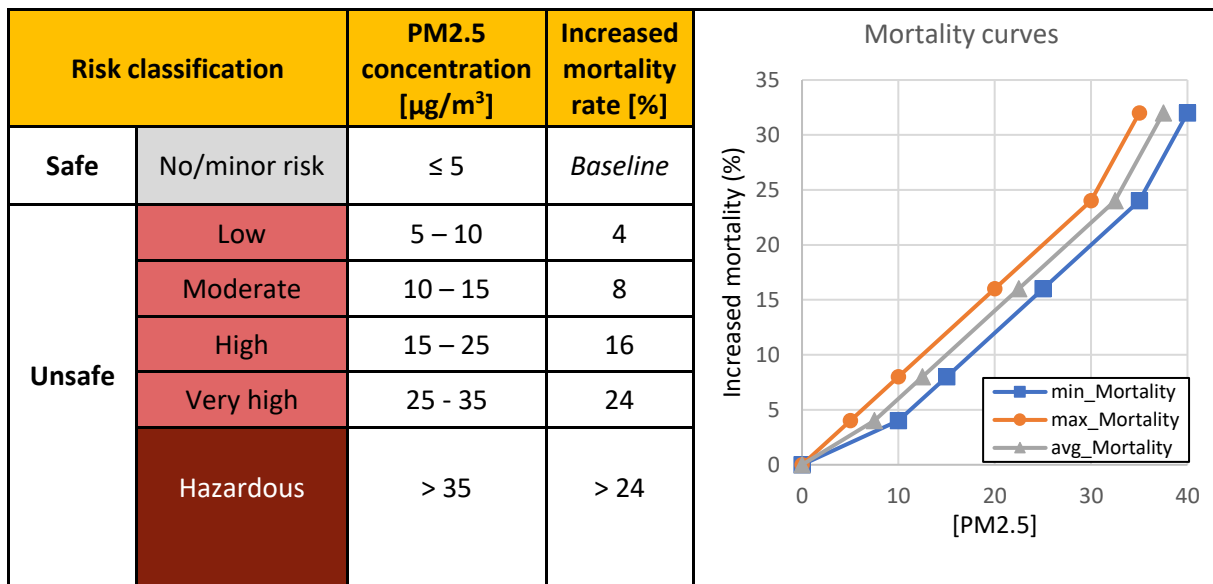
10.4 Heat stress

Population: standard heat stress classification ([Blazejczyk et al. 2012](#)) for Wet-Bulb Globe Temperature (°C).

WBGT (°C)	Stress category (population)
> 30	Extreme heat
28 to 30	Intense heat
23 to 28	Strong heat
18 to 23	Moderate heat
<18	No thermal stress

10.5 Air pollution

Population: mortality function in relation to PM2.5 concentration. Risk classes according to [WHO Air Quality guidelines \(2021\)](#).



10.6 Tropical Cyclones

Built-up: A regionalised sigmoidal function is applied in this report, as described in [Eberenz et al., 2020](#).

